RIFT BRITTLE STRUCTURE, PRECAMBRIAN DUCTILE STRUCTURE, AND CRUSTAL THICKNESS VARIATION WITHIN AND AROUND THE CENOZOIC MALAWI RIFT

By

KATHLEEN E. ROBERTSON

Bachelor of Science in Geology

Brigham Young University

Provo, UT

2013

Submitted to the Faculty of the
Graduate College of the
Oklahoma State University
in partial fulfillment of
the requirements for
the Degree of
MASTER OF SCIENCE
December 2020

RIFT BRITTLE STRUCTURE, PRECAMBRIAN DUCTILE STRUCTURE, AND CRUSTAL THICKNESS VARIATION WITHIN AND AROUND THE CENOZOIC MALAWI RIFT

Thesis Approved:

Dr. Mohamed Abdelsalem

Thesis Adviser

Dr. Estella Atekwana

Dr. Daniel Laó Dávila

Name: KATHLEEN E. ROBERTSON

Date of Degree: December 2020

Title of Study: INVESTIGATING THE INFLUENCE OF PRE-EXISTING STRUCTURES ON RIFT EVOLUTION AT THE SOUTHERN TERMINATION OF THE MALAWI RIFT

Major Field: GEOLOGY

Abstract:

This study examines the relationship between the regional brittle structure associated with the Cenozoic southern Malawi Rift and the surrounding ductile structure of the Precambrian crystalline basement, as well as the controls of the Precambrian ductile structure and crustal thickness variation on rift brittle structure.

The southern Malawi Rift is characterized by a sharp change in orientation from NNW-trending in the north to NE-trending to the south before terminating against the Paleozoic – Mesozoic Shire Graben. Shuttle Radar Topography Mission (SRTM) Digital Elevation Models (DEM) and RADARSAT are used to map the rift brittle structure whereas aeromagnetic images are used to map Precambrian ductile structure. Variations in crustal thickness are obtained from previously published study that used two-dimensional radially-averaged power spectral analysis of the World Gravity Model 2012 (WGM 2012) to map the Moho depth beneath the southern Malawi Rift and its surroundings. After manually extracting the fault orientations for both the surface and basement structures, the data were divided using geophysical trends in the basement complex to create six structural domains. Each domain was applied over the same geographic area to examine structural inheritance within rift structures using rose diagrams for frequency analysis.

Within the study area, the brittle rift structures do not always correspond with the fabric of the basement complex and, in some cases, show only a minor relationship. The surficial structures react to pre-existing weaknesses in three ways: 1) follow the dominate trend of basement anisotropies; 2) cut across all basement anisotropies; or 3) have at least one trend that follows basement anisotropies and one or more trends that do not follow basement structures.

Crustal thickness data were also analyzed to examine the influence of crustal thickness heterogeneity on current rift structure. In the study area, crustal thickness seems to be a primary control for rift location and propagation and may correspond to the Niassa Craton underlying parts of the Southern Irumide Belt west of the study area. However, if the pre-existing structures are favorably oriented, and severe crustal heterogeneity is absent, the rift will follow established basement structures.

TABLE OF CONTENTS

LIST OF FIGURES

LIST OF FIGURES

Figure Page

CHAPTER I

INTRODUCTION

Continental rift systems are complex three-dimensional structures that evolve through a series of geodynamic processes (e.g. Corti et al., 2007; 2013a and b; Corti, 2012). These structures are predicted to be delineated by brittle structure in the upper crust and underlain by thinned crust and sub-continental lithospheric mantle (SCLM) attributable to lithospheric stretching (e.g. Olsen, 1995; Thybo and Nielsen, 2009). Thinning of the SCLM allows for the upwelling of the asthenosphere, which supplies magma to be injected in the upper crust in the form of mafic dikes that thermally soften the lithosphere, reducing the required tensile stress required for its stretching (e.g. Buck, 2006; Schmeling, 2010). This "magma-assisted rifting" process might be best exemplified by the magma-rich Afar Depression and the Main Ethiopian Rift, which represent the northern segments of the East African Rift System (EARS) (Fig. 1A; e.g. Ebinger, 2005; Kendall et al., 2005). This magma-rich segment continues southward into the Eastern Brach of the EARS (Fig. 1A; Koptev et al., 2015, 2018).

While "magma-assisted rifting" explains the behavior of many segments of the EARS, it has been documented that the Western Branch of the EARS (Fig. 1A) is largely amagmatic (e.g. Koptiv et al., 2015; 2018). The lack of magma-assisted rifting in the Western Branch of the EARS brings into question the controls necessary for amagmatic rift processes. Structures associated with magma-poor continental rift systems, such as the Western Branch of the EARS,

often inherit the geometry of pre-existing structures formed during the tectonic evolution of the pre-rift orogenic belts, largely Paleoproterozoic to Neoproterozoic in age (e.g. Delvaux, 1989; Daly et al., 1989; Delvaux et al., 1992; Morley, 1999; Morley et al., 2004; Van Wijk, 2005; Corti et al., 2007; 2013; Katumwehe et al., 2015; Leseane et al., 2015; Sarafian et al., 2018; Heilman et al., 2019). Although significant advances have been made in understanding the first order controls of the pre-existing Precambrian crystalline basement structures (henceforth Precambrian ductile structure) in the localization of extensional strain during the onset of continental rift systems and their subsequent emerging geometry, only few studies have focused on understanding the geometrical relationship between the Precambrian ductile structures and the regional pattern of the brittle structure, namely regional fracture, associated with continental rift systems (henceforth rift brittle structures). Some studies (e.g., Daly et al., 1989; Morley, 1999; Michon and Sokoutis, 2005; Misra and Mukherjee, 2015) suggested that there are two factors that determine whether the rift brittle structures will activate the pre-existing structure: (1) the angle between the orientation of the pre-existing structures and the direction of the maximum tensile stress and (2) the difference between the mechanical strength of the pre-existing structures and the mechanical strength of the surrounding rock mass. It has been shown that pre-existing structures that are oriented between 15° and 45° to the direction of the maximum tensile stress will be reactivated by the rift brittle structures (Misra and Mukherjee, 2015). In addition, some studies addressed the deviation of the trend of rift border fault from following pre-existing structures (e.g., Versfelt and Rosendahl, 1989; Ring 1994; Michon and Sokoutis, 2005). These studies attributed this deviation to lack of favorable angle between the orientation of the pre-existing structures and the direction of the maximum tensile stress and that this deviation contributes to rift segmentation.

The relative role of the Precambrian ductile structures and variation of crustal thickness in the localization of extensional strain and the spatial distribution of the rift brittle structure remain poorly-understood. Tomassi and Vauchez (1998) proposed that on a continental scale, mechanical behavior in a continental rift system is more likely to be influenced by SCLM rheology, while on a small scale, mechanical behavior is largely influenced by pre-existing structures. Generally, it is suggested that the mechanical behavior of a continental rift system in the upper crust is strongly controlled by the rheology of the crust that is influenced by the presence of thermal anomalies and compositional and thickness heterogeneity of the crust (e.g., Leseane et al., 2013). For example, Tommasi and Vauchez (2001) suggested that rheological variation within the relatively thick and warm crust of orogenic belts can significantly reduce the mechanical strength of the lithosphere, allowing for extensional strain localization during the onset of continental rift systems. This is further supported by numerical and analogue modeling such as those presented by Corti et al. (2007) that illustrated the development of the northern part of the Western Branch of the EARS within the Paleozoic – Mesozoic orogenic belt at the western margin of the Archean – Paleoproterozoic Tanzanian craton (Fig. 1A).

However, this is not representative of all segments of the EARS. The Malawi Rift, which represents the southern termination of the Western Branch of the EARS is oriented N-S (Fig. 1A and B) and does not follow the margins of any Archean – Paleoproterozoic craton and it cuts obliquely across Precambrian and Paleozoic - Mesozoic rift basins of different orientations (Castaing, 1991; Delvaux et al., 1992; Chorowicz, 2005; Laó Dávila et al., 2015). Because the rift brittle structures of the Malawi Rift, in many places crosses the Precambrian ductile structures and brittle structures of the Paleozoic – Mesozoic rift basins, some studies

debated the role of pre-existing structures in promoting extensional strain localization (e.g. Ebinger et al., 1987; 1989).

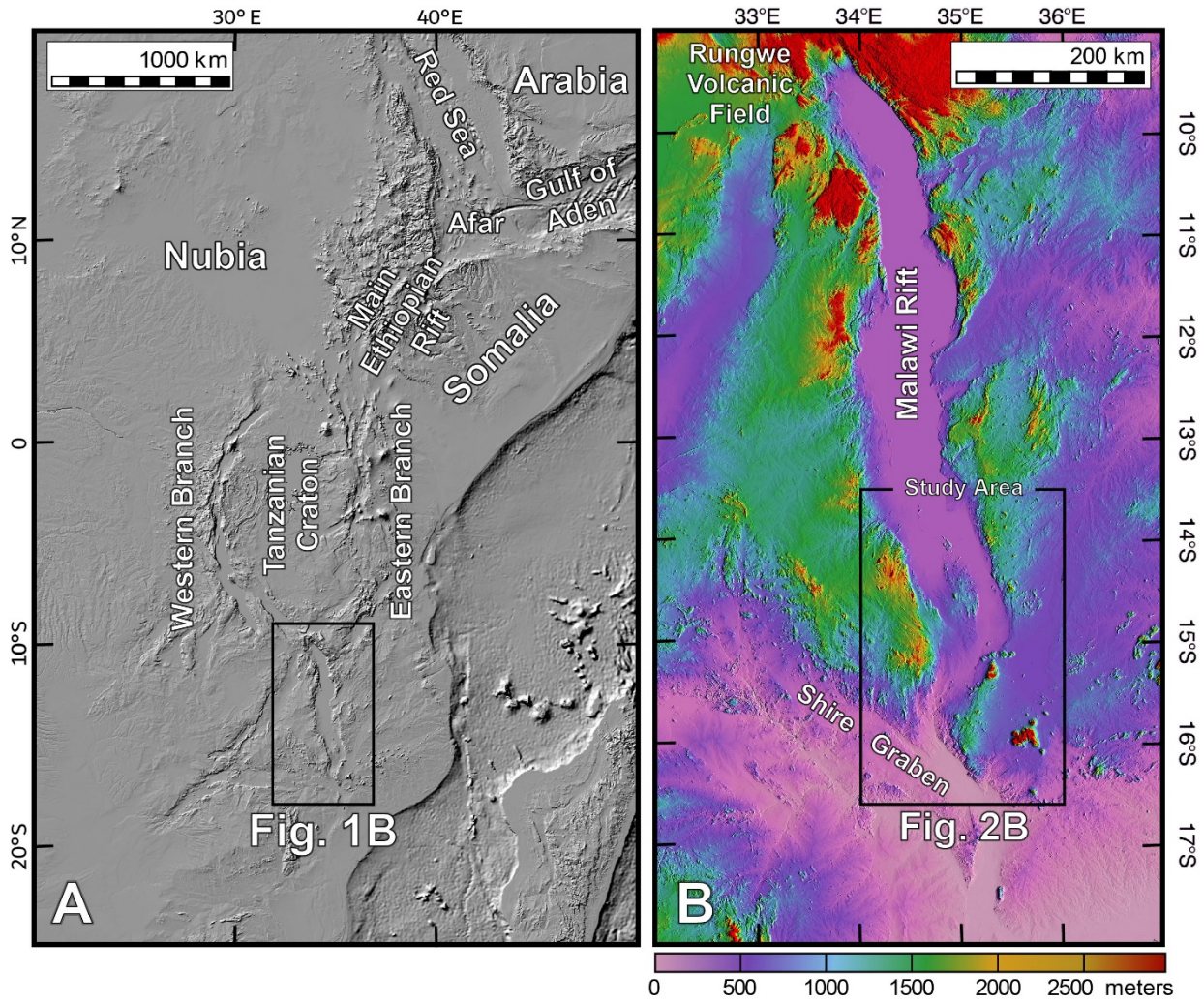

Figure 1: (A) Earth Topography 1 arc second (ETOPO1) Digital Elevation Model (DEM) (1 km spatial resolution) of the East African Rift System (EARS). The black box with Fig. 1B below it provides the general geographic extent of Malawi. (B) Shuttle Radar Topography Mission (SRTM) DEM (90 m spatial resolution) of the Malawi Rift with the study area outlined.

This study examines the relationship between the regional rift brittle structures (including the rift border faults) and the Precambrian ductile structures in the southern Malawi Rift as well as the relationship between the spatial distribution and orientation of these structures to the variation in crustal thickness. (1) Enhanced Shuttle Radar Topography Mission (SRTM) Digital Elevation Model (DEM) and RADARSAT images are used to map the spatial distribution and orientation of the rift brittle structures. (2) Enhanced aeromagnetic images are used to map the spatial distribution and extent of Precambrian ductile structures. (3) Both the rift brittle structures and the Precambrian ductile structures are divided into a number of structural domains that have common structural styles and orientations. (4) The general orientations of the rift brittle structures and the Precambrian ductile structures within each structural domain are documented through rose diagrams in order to facilitate the comparison between the two structural sets. (5) The regional distribution, structural style and orientation of the rift brittle structures and the Precambrian ductile structures are compared with crustal thickness variation which is obtained from Moho depth imaging using two-dimensional (2D) radially average power spectral analysis of the World Gravity Model 2012 (WGM 2012) (Njinju et al., 2019).

CHAPTER II

TECTONIC SETTING

2.1 Tectonic setting of the Malawi Rift

The Malawi Rift marks the southern termination of the Western Branch of the EARS (Fig. 1A and B). The rift extends in a general N-S direction from the Pliocene – Pleistocene Rungwe volcanic province in the north (the only location where there is surface volcanism) to the Paleozoic – Mesozoic Shire Graben to the south (Fig. 1B).

There is debate regarding the actual termination location of the Malawi Rift. The main rift extends for at least 700 km to the Shire Graben (Fig. 1B, 2A and B). However, there is a suggestion that the Malawi Rift continues further south and terminates in the Urema Graben in Mozambique **(**Figure 1A; Ebinger et al, 1987; Delvaux, 1992; Ring et al., 1992; Ring, 1994). Previously, the initiation of the Malawi Rift was suggested to be at ~8.6 Ma as shown from $^{40}Ar/^{39}Ar$ age dating of rocks from the Rungwe volcanic province (Ebinger et al., 1993). However, a more recent $^{40}Ar/^{39}Ar$ age dating of rocks from the Pungwe volcanic province gave older ages ranging between 18.5 Ma and 17.6 Ma (Mesko et al., 2014) suggesting that the age of volcanism is older than tectonic extension.

Because of the structural variation within the rift floor and border faults, Ebinger et al. (1987) proposes that the Malawi Rift should be divided into the Karonga, Nkhata, Nkhotakota, Monkey Bay, and Shire sections (Fig. 2A). Laó Dávila et al. (2015) proposed first-order and second-order hierarchal segmentation for the Malawi Rift. The first-order segmentation divides

the Malawi Rift on a regional scale into northern, central, and southern sections (Fig. 2A). In the northern section, the Malawi Rift largely follow Paleoproterozoic – Neoproterozoic structures, but the rift cuts through Mesoproterozoic – Neoproterozoic structures in its central section. Additionally, the Malawi Rift within its northern and central sections is filled with the ~550 km long Lake Malawi that is underlain by Cenozoic sedimentary rocks ranging in thickness between ~1 km and ~2 km (Specht and Rosendahl, 1989). The second order segmentation of in the northern and central sections of the Malawi Rift is represented by the presence of four half-grabens or asymmetrical grabens with alternating polarity, separated with what is termed "flip-over full-grabens (Fig. 2A; Laó Dávila et al., 2015).

Using the first-order segmentations to examine the Malawi Rift border fault systems suggests the rift tip propagated as a single unit in the Northern Section, occupying a narrow zone of rift localization and causing a pronounced vertical displacement within rift shoulders of up to ~1,500 m (Ebinger, 1987; Flannery and Rosendahl, 1990). The northern border faults were strongly influenced by the N-NW trends emplaced by the Paleoproterozoic-age Ubendian Belt (Chorowicz and Sorlien, 1992; Laó Dávila et al., 2015). Favorably oriented structures facilitated strain localization that was used by many Malawi Rift border fault segments through either reactivation or planes of weakness (Flannery, 1990; Castaing, 1991; Chorowicz, 2005; Fritz et al., 2013). The Central Section primarily consists of folded Precambrian fabric, which enables the rift tip to use regional structural trends instead of inherited lithospheric heterogeneity. South of the Central Section, the rift tip encounters the stronger lithosphere of a well-developed horst, the Shire Horst. This causes the rift to splay, bifurcating into the Makanjira Trough and the Malombe Graben (Fig. 2A; Njinju et al., 2019).

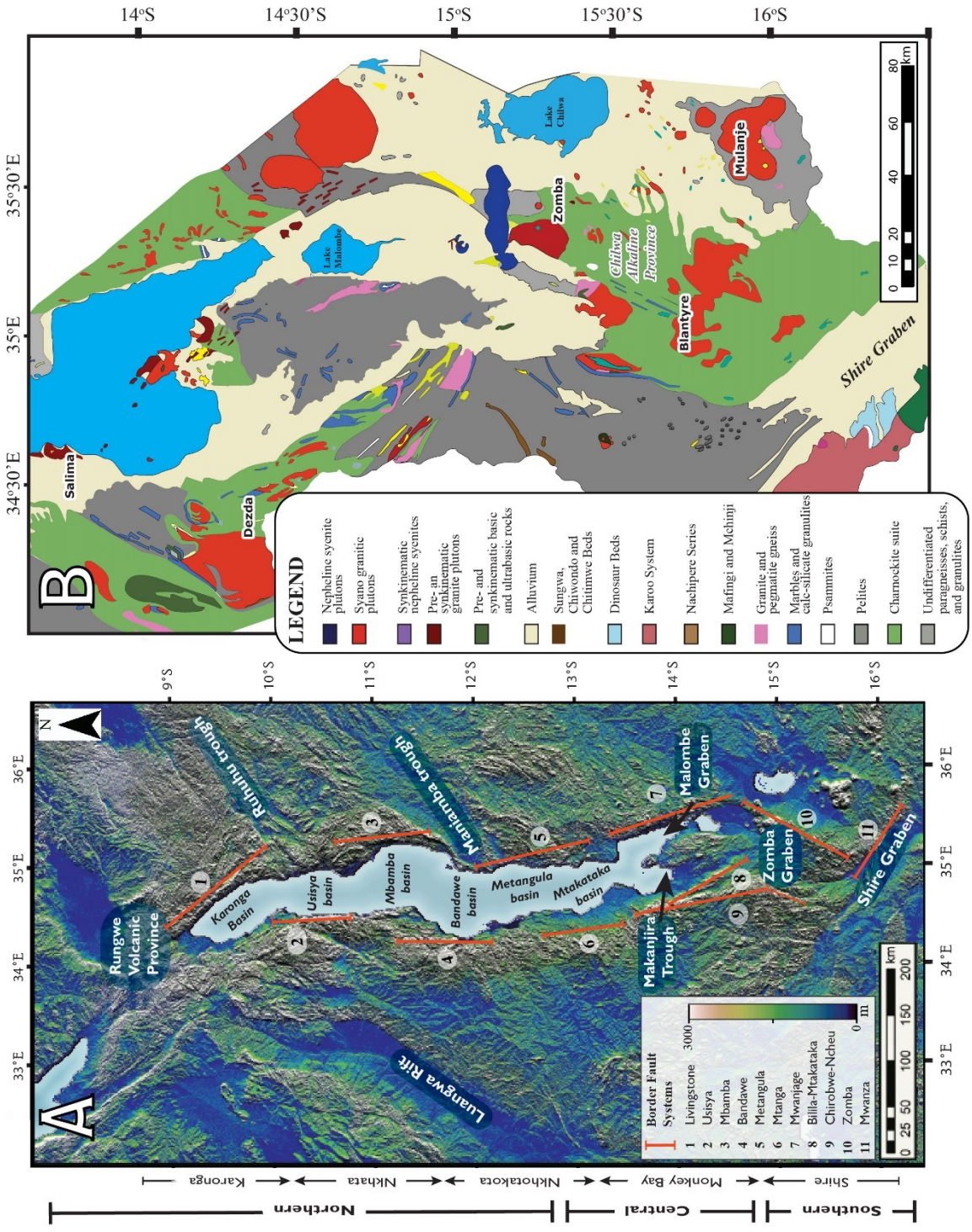

Figure 2: A) Shuttle Radar Topography Mission (SRTM) Digital Elevation Model (DEM) of the Malawi Rift and surrounding features labelled. The Northern, Central, and Southern divisions are based on Laó Dávila et al. (2015) based on hierarchal segmentation. The Karonga, Nkhata, Nkhotakota, Monkey Bay, and Shire are based on Ebinger et al. (1987). B) A geologic map over the study area with the main lithology labelled, based on Bloomfield, K. et al. (1966).

In the Southern Section, the border fault systems characteristically have less defined, curvilinear escarpments with wide-spread rift shoulders that are not as restrictive as in the northern border fault system. The Malawi Rift is truncated against the unfavorably oriented NW-striking Shire Graben (Castaing, 1991; Chorowicz, 2005).

2.1.1. Pre-rift basement structure of the Malawi Rift

The structures within and around the Malawi Rift are derived from multiple origins, including the Precambrian and Pan-African orogenic belts, late-Paleozoic to Mesozoic Karoo sedimentary basins, and shear zones (Fig.2A and B; Castaing, 1991; Delvaux, 2001; Catuneanu et al., 2005; Chorowicz, 2005; Fritz et al., 2013). Like other EARS rift segments, the architecture of the Malawi Rift is characterized by alternating, asymmetrical half-grabens of opposing polarity. (Fig. 2A; Specht and Rosendahl, 1989; Flannery and Rosendahl, 1990; Mortimer et al., 2007; Hodge et al., 2014). Six major basins are identified within the Malawi Rift: the Karonga, Usisya, Mbamba, Bandawe, Metangula, and Mtakataka basins (Ebinger et al., 1987; Specht and Rosendahl, 1987; Chapola and Kaphwiyo, 1992). Each basin is bound by at least one border fault system (Fig. 2A). The Malawi Rift border faults define the rift and control the overall basin development, which confines rift locale and propagation. Despite the controls on rifting, the geometric relationship between pre-rift basement and border fault systems varies along-strike relative to the rift (Fig. 2A; Contreras, 1990; Flannery and Rosendahl, 1990; Ring, 1994).

2.2 Kinematics of the Malawi Rift

The extension direction of the Malawi Rift remains debatable. Although current results of kinematic analysis indicate orthogonal extension in the E-W direction, slickenlines and fault striations indicate rifting may have shifted from a predominately oblique system to

the current orthogonal system. Sinistral lateral stepping and obliquely oriented faults and sub-basins further elucidate this shift (Mortimer et al., 2007; Laó Dávila et al., 2015).

Saria et al. (2014) built upon previous studies by Stamps et al. (2008) and Calais et al. (2006) by using data compiled from Global Position System (GPS) resources, earthquake records, and transform fault azimuths to model present-day kinematics along the EARS. The model predicts a rate of 2.2 mm/year in the northern portion, decreasing to 0.8 mm/year in the southern portion of the Malawi Rift. The model proposed by Saria et al. (2014) predicts extension in the E-W direction. This model is supported by Sander and Rosendahl (1989), Morley (1989), Morley et al. (1992), and Fairhead and Stuart (1982). Versfelt and Rosendahl (1989) used seismic data collected by Project PROBE to suggest a NW-SE direction of extension, which is supported by Piper (1989), Delvaux et al. (1992), Mondeguer et al. (1989), and Chorowicz et al. (1987). Ebinger (1989) used fault striations and micro-kinematic structures to conclude extension is NE-SW in direction, while Castaing (1991) suggests a minor NE-SW direction of extension and a major NW-SE trend. Ring (1994) suggests three phases of extension determined largely through cross-cutting relationships. In the initial stage, extension in the ENE-WSW direction reactivated structures-oriented NW to NNW. During the second stage, extension directions rotated into an E-W oriented extension that reactivated dip-slip faults into strike-slip and oblique-slip faults. The third stage emplaced N to NE-striking faults with an ESE to SE direction of extension.

Most current studies suggest the Malawi Rift propagated north to south, though the paucity of data between the Malawi Rift and the Urema Graben make this hypothesis difficult to ascertain. This model of rift opening is supported by gravity data and lacustrine core analysis, which indicate basin subsidence and sediment accumulation are greatest in the north and

decreases southward (Flannery and Rosendahl, 1990; Ebinger, 1993; Ring, 1994; Scholz et al., 2007). Previous studies postulate rift valleys should narrow with decreasing age (Ring et al., 1992; Mortimer et al., 2007). This is not the case in the Malawi Rift, where the northern and southern tips of the Malawi Rift are almost equal in width, which indicates strain is accommodated elsewhere, or that the propagation of the rift is not N-S (Laó Dávila et al., 2015). Southern Malawi lacks significant surface deformation, but it does exhibit characteristics of rift termination, including bifurcation of the rift valley and diffuse border fault systems. A change in strain accommodation is discernable by examining the elevations of the rift shoulders, which change from 1,500 m in the north to 250 m where the rift truncates against the Shire Graben.

2.3 Study area in southern Malawi

In the Central and South Sections of the Malawi Rift, weaknesses and anisotropies in the basement often influence border fault development and rift architecture, but do not conform closely to proposed rift models. Consequently, no consensus is apparent to the controls constraining rift propagation in southern Malawi. The rift architecture of the Malawi Rift has been studied using field methods, seismic data, and composite research (e.g., Versfelt and Rosendahl, 1987; Ebinger et al., 1987 Delvaux et al., 1992; and Ring, 1994; respectively). The study area is limited to southern Malawi (Fig. 1B and 2B), specifically the Central and the South Sections defined by Laó Dávila et al. (2015) to identify the controls of strain localization and mechanical inheritance on rifting near the termination of the Malawi Rift (Fig. 2A).

The northern tip of the rift, near the Rungwe Volcanic Province (Fig. 2A), occupies a narrow zone of rift localization, and some studies suggest that strain is accommodated primarily within the high shoulders of the border faults (Ebinger et al., 1987; Ring and Betzler,

1995). The Central and South Sections of the Malawi Rift differ by exhibiting a more diffused strain distribution system with low, wide-spread rift shoulders and multiple border fault systems.

In the Central Section, most of the surface structures strike NW and NE (Castaing, 1991; Laó Dávila et al., 2015). The rift is still controlled predominately by inherited structures and propagates as a single unit, until it bifurcates around the Shire Horst to form the Makanjira Trough and Malombe Graben (Fig. 2A; Dulanya, 2017). The western Makanjira Trough has experienced less subsidence and is ~50 km wide, with a less developed border fault, the Bilila-Mtakataka fault, bounding it to the west (Fig. 2A). This trough is contrasted by the deeper, more developed eastern Malombe graben, which is narrower (~20 km) and deeper than the Makanjira Trough, with two bounding faults – a small fault along Monkey Bay and the main border fault, the Mwanjage fault (Fig. 2A; Laó Dávila et al., 2015; Dulanya, 2017). Fig. 2A shows the locations of the basins and main border fault systems. Where the Malombe graben terminates, the orientation of the eastern border fault system (Mwanjage) abruptly changes 116° from NNW to NE-striking, leaving the Shire Horst striking in the NNW direction (Fig. 2; Laó Dávila et al., 2015). The border fault systems in this region obliquely cut many of the pre-existing surface structures and strongly foliated basement rock.

Although most of the interior rift structures south of the Shire Horst are covered by Quaternary sediment, a well-defined strike-slip fault system crosses the southern Malawi Rift. The wrench fault system is formed by a series of ENE- to NE-trending faults that were intruded by Precambrian infra-crustal ring complexes in the Precambrian era and later by the Chilwa Alkaline Province magmatism (Fig. 2B; Dulanya, 2017).

The Shire Graben is in southern Malawi, a NW-trending graben bound by the Mwanza and Thyolo faults in the northeast. The Lengwe and Mwabvi basins are located within the Shire

Graben and correspond to a transtensional zone that formed principally because of these sinistral pre-transform NW-SE faults (Flannery and Rosendahl, 1990; Castaing, 1991).

2.4 Geology of southern Malawi

Outcrops in southern Malawi predominately consist of crystalline, high-grade metamorphic basement rock. The Malawi Rift is positioned within the remnants of Proterozoic mobile belts, which created a complex basement fabric that is strongly foliated and altered by several tectonic events. The basement rock was emplaced during the Proterozoic orogenesis that formed the Irumide and Southern Irumide belts and caused formation of NE-trending features in southern Malawi, most noticeably the regional shear zones that cross-cut the basement fabric (Daly, 1989; Piper, 1989; Fritz et al., 2013).

Another event that altered the basement in southern Malawi was the Paleozoic-age Pan-African Orogeny, which occurred during the assembly of Gondwana and concluded ~500 Ma (Flannery and Rosendahl, 1990; Castaing, 1991; Eby et al., 1998; Kröner et al., 2001; Dill, 2007). Structures formed from the Pan-African Orogeny followed two trends: the NE-trend imposed during the Proterozoic, and as a lesser NW-trend during a period of intense brittle deformation (Flannery and Rosendahl, 1990; Eby et al., 1998; Kröner et al., 2001; Dill, 2007). The interaction between the different orogenies created a chaotic basement fabric within the southern rift valley, which allows the Malawi Rift border fault systems to follow the pre-existing basement and surface trends in some areas and transect the pre-existing structures in other areas (Castaing, 1991; Delvaux, 1992).

Laterally extensive sedimentary rock units belonging to the Karoo system were established during the late Paleozoic-Jurassic and cover portions of the exposed basement in

southern Malawi (Ring, 1995). The Karoo system emplaced multiple NW- and NE-trending troughs and valleys, including the Luangwa Rift, and the Ruhuhu and Maniamba troughs (Fig. 2A; Chorowicz, 1987; Castaing, 1991; Laó Dávila et al., 2015). Within the rift itself, fluvial and lacustrine sediments fill the basins, obscuring the Precambrian formations (Castaing, 1991; Kreuser, 1995; Chorowicz, 2005; Dill, 2007, Dulanya, 2017).

Periods of magmatism during the Mesozoic Era stimulated thermal uplift and altered the composition of the lithosphere, and led to magmatic events, beginning with volcanic plugs and ring complexes within the Chilwa Alkaline Province, during the Jurassic and Cretaceous (2B; Woolley, 1979; Eby et al., 1995, 2004). This province encompasses a large portion of southern Malawi, before extending into Mozambique, and Zambia (Woolley, 1991). During this magmatic sequence, widespread intrusions of carbonatite, ijolite, nepheline syenite in the form of plutons and ring complexes transfigured the landscape and altered the basement fabric. The largest ring complex is south of Lake Malawi, Mt. Mulanje, which rises 3,000 m from the level Palombe Plain (Woolley, 1991; Eby et al., 1995). Formation of these large intrusions was followed by formation of smaller syenite plutons and alkaline dike swarms, oriented primarily NE (Castaing, 1991). In the lower Jurassic, Stormberg Volcanic events emplaced NE-trending dolerite dikes and sills, primarily during basaltic eruptions likely activated by faulting (Fig. 2B; Eby et al., 1995, 2004; Woolley, 1979). The extrusions and plutons from the Chilwa Alkaline Province conceal or alter basement fabric to the southeast of Lake Malawi, contributing to the chaotic nature of the Central and Southern Sections (Fig. 2; Woolley et al., 1979; Woolley, 1991; Eby et al., 1995).

CHAPTER III

DATA AND METHODOLOGY

This study used the National Aeronautics and Space Administration (NASA) Shuttle Radar Topography Mission (SRTM) Digital Elevation Models (DEMs) and RADARSAT, coupled with aeromagnetic data, to assess the role played by heterogeneity within the crust on extensional strain localization and rift termination in the southern Malawi rift. Different filtering techniques were used on the SRTM DEM, RADARSAT data, and aeromagnetic to enhance the interpretability of the ductile and brittle structural fabric associated with the Precambrian basement and the Cenozoic southern Malawi rift. Subsequently, the ductile Precambrian basement and Cenozoic rift structures location and strike of the surface structures and basement anisotropies, comparisons were made of the degree of structural offset, rift segmentation, and rift tip interaction with pre-rift structures to examine the influence Precambrian anisotropies and lithospheric heterogeneity have on influencing rift termination.

3.1. Shuttle Radar Topography Mission (SRTM) Digital Elevation Model (DEM) processing

The Consortium for Spatial Information (CGIAR-CSI) provided 3-arc-second SRTM DEM data with 90 m spatial resolution. Edge-detection filters were applied to the SRTM DEM using Geosoft Oasis montaj™ software to improve the visual interpretation of the brittle structure associated with the southern Malawi rift (Fig. 3). Image processing techniques often

use mathematical transformations to extract information that raw images do not readily exhibit. Image analysis employed using the Fourier transform, one of the more popular transformations, is unconventional for DEM processing, but can be helpful in interpreting surface features. Applying Fourier transformation to elevation data allows more efficient image processing when smoothing or sharpening an image (Dougherty, 2009; Jepson, 2005; Toth et al., 2014). This transformation enables one surface to be represented in multiple domains. In the spatial domain, the surface is encoded as brightness as a function of spatial displacement obtained from raw image data. However, in the Fourier domain, the surface is represented through a summation of a series of sinusoids in terms of amplitude as a function of frequency (Cooper and Cowan, 2004; Lehar, 1999; Jepson, 2005).

Applying the first vertical derivative to the SRTM data highlights magnetic highs and edges. The software uses the information encoded in the Fourier domain and calculates the derivative of the two-dimensional function representing the surface. The high-pass filter reduces the influence of longer wavelengths, thereby improving the resolution of superimposed rift structures (Lehar, 1999; Dougherty, 2009). While useful for surface lineation mapping, the data obtained from extracting the vertical derivative are not physically meaningful. The first vertical derivative of the DEM measures only relative elevation, losing the value of the absolute elevation during the derivative process (Cooper and Cowan, 2004; Lehar, 1999; Jepson, 2005; Toth, 2014). Filtering techniques to emphasize linear structures in both the x-direction and the y-direction followed a similar process. Hillshades with a z-factor of 0.00000935 were produced using Exelis Visual Information Solutions (ENVI) software to emphasize surface structures. Different maps emphasized unique trends. For example, the crisp hillshade is often able to resolve smaller details than the horizontal derivative. However, the horizontal

derivative can emphasize trends visually unnoticed in the hillshade. The visual interpretation of the SRTM DEM that is enhanced by the edge-detection filter produced structural maps representing the brittle structure associated with the southern Malawi rift (Fig. 3).

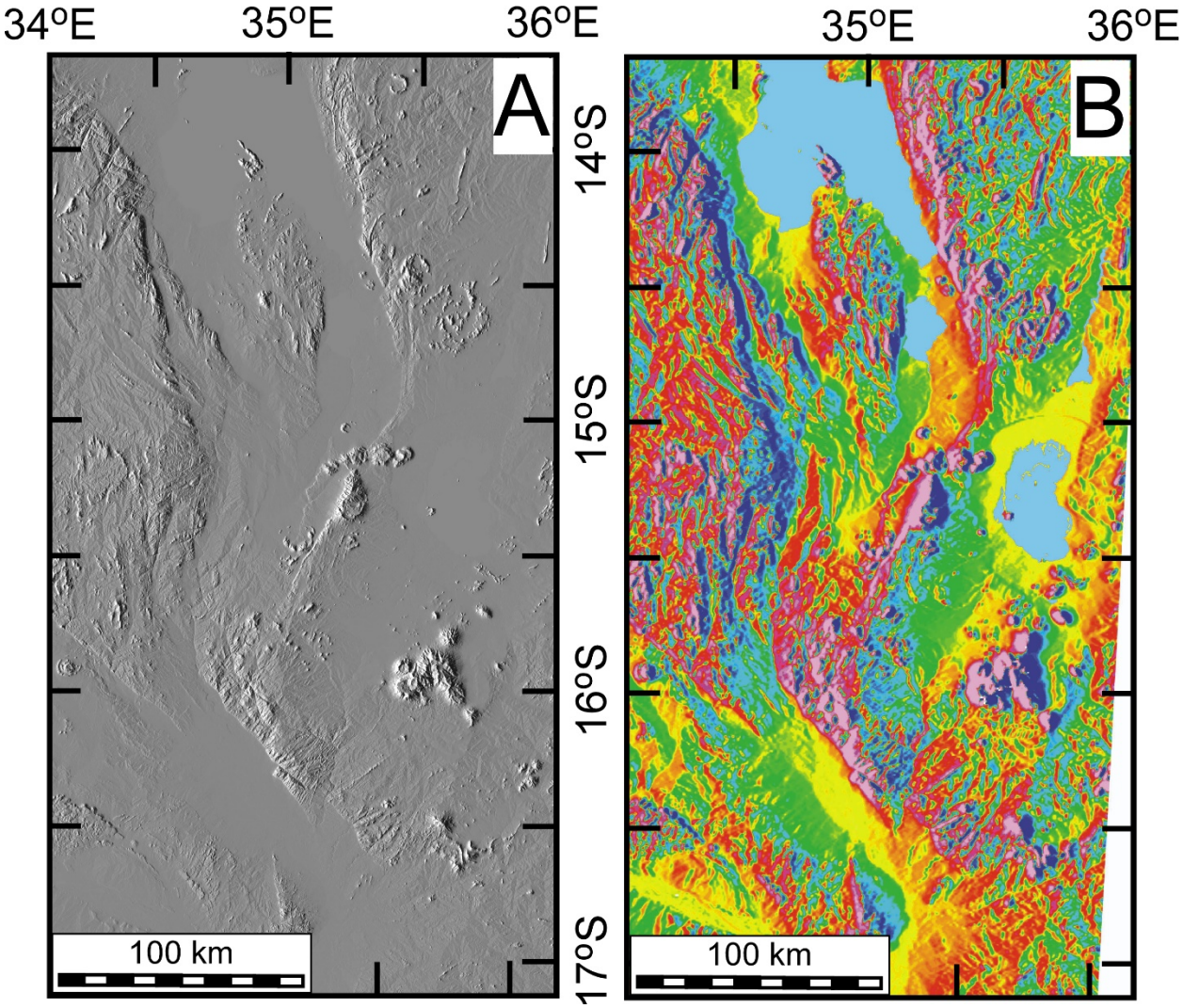

Figure 3: A) Grayscale Shuttle Radar Topography Mission (SRTM) Digital Elevation Model (DEM) of southern Malawi. B) Enhancing of the brittle structure associated with the southern Malawi Rift shown in the greyscale SRTM DEM with color-coded hillshade and horizontal derivative filtering in the x-direction (Dx).

3.2. RADARSAT data processing

Often RADARSAT data present a clearer view of surface structures, particularly in regions with varying lithology or deformation style, while DEMs extracted from SRTM data are useful for measuring changes in elevation (Fig. 4). RADARSAT is a space-borne radar system of the Canadian Space Agency (CSA). RADARSAT has 30 m spatial resolution and uses standard beam data collected from 798 km in elevation at a 98.6° inclination with a 45° look angle, using Synthetic Aperture Radar equipment. The RADARSAT satellite generates images of the Earth by transmitting microwave energy and recording the backscattered signals. RADARSAT is sensitive to changes in terrain and surface roughness, yielding detailed images of brittle surface structures and folds (Fig. 4).

Noise reduction without losing the integrity of the data was an important consideration when processing the RADARSAT images over the southern Malawi rift. Three filters reduced noise and sharpen structural features and illustrated the contrast in surface roughness: 1) a 2% linear stretch, which sharpens features by eliminating 2% of the high and low data values; 2) an Enhanced Lee filter, which uses local statistics to reduce noise while still preserving textural information; and 3) an Laplacian filter, a second derivative edge enhancement filter (Fig. 4).

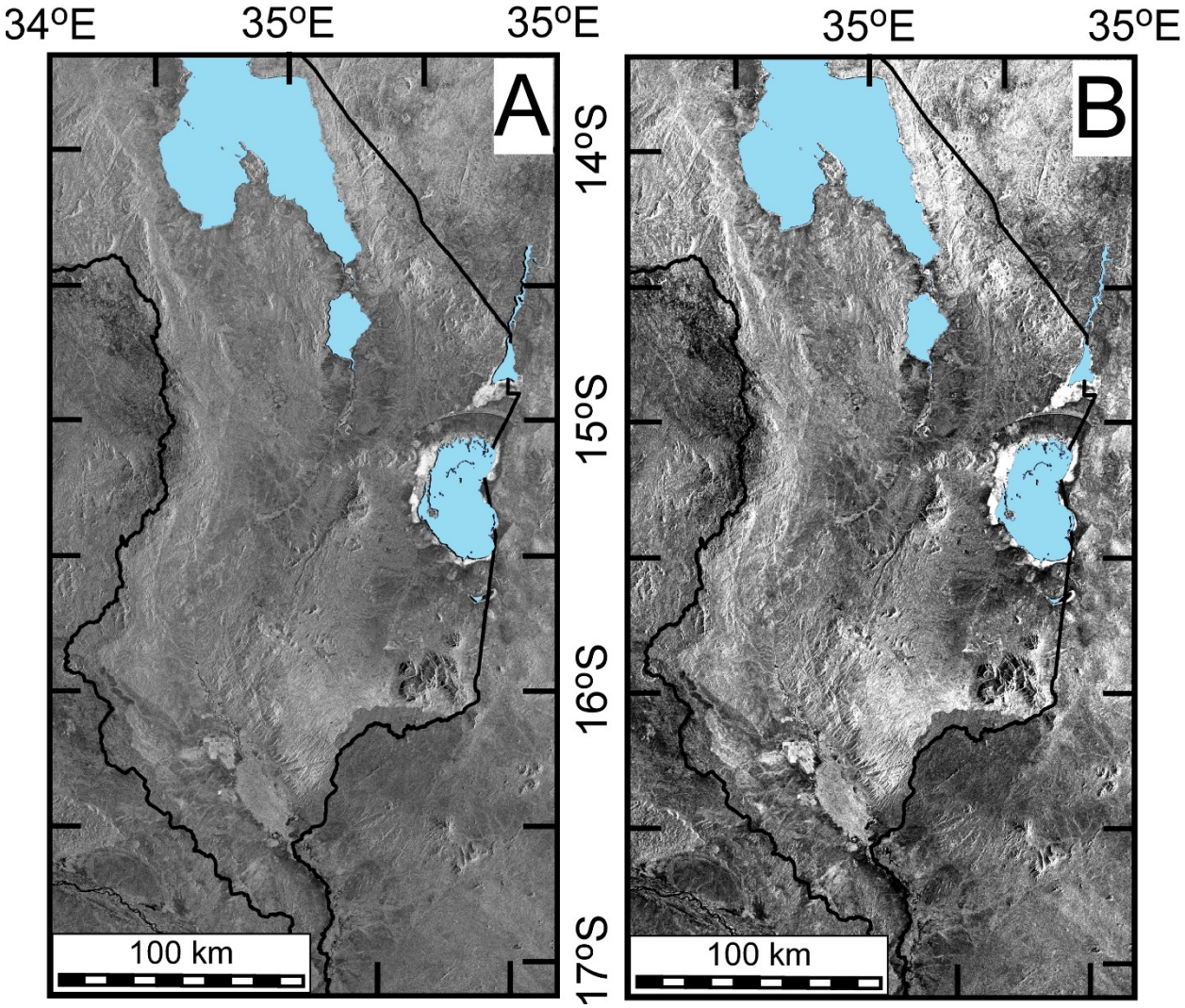

Figure 4: A) Unfiltered RADARSAT data over southern Malawi. B) RADARSAT data with three primary filters to reduce noise and sharpen linear structural features: 1) a 2% linear stretch that eliminates 2% of the high and low data values; 2) an Enhanced Lee filter to reduce noise, and 3) an Laplacian filter, a second derivative edge enhancement filter.

3.3. Aeromagnetic data processing

High- and low-resolution aeromagnetic data, obtained from the Malawi Department of Geologic Survey were used to map the ductile structure associated with Precambrian crystalline basement surrounding the southern Malawi rift. Data collected were acquired at a constant terrane clearance of 60 m and post-processed using draped field computations. The surveys were collected along NE-SW-oriented transverse lines spaced 250 m apart. The low-resolution aeromagnetic data were acquired between 1984 and 1985, by Hunting Geophysics of Canada) from an altitude of 250 m using a line spacing of 1 km and 10 km tie-lines.

Filters applied using Geosoft Oasis montaj™ software (Geosoft, 2010**)** produced Total Magnetic Intensity images showing the degree of magnetization and magnetic anomalies (Fig. 5). Upward continuation of the magnetic survey applies mathematical formulas to project data to higher elevations (200 m), which smooths the data by reducing the high-frequency wavelengths that result from surface noise (Ganiyu et al., 2012). Interpolation by the minimum curvature method further enhanced the dataset, smoothing and filling gaps in the data (Briggs, 1974). Individual application of other filters - the first vertical derivative, horizontal derivatives, tilt derivative, and the analytical signal - were used to accentuate near surface structures. The first vertical derivative removes long-wavelength aspects of the magnetic field, sharpening the resolution of regions with superimposed structures (Fig. 5; Cooper and Cowan, 2004). The horizontal derivatives in the x (Dx) directions emphasizes structures oriented N-S and in y (Dy) direction it emphasizes structures oriented E-W, accentuating sharp changes in physical properties by comparing lateral variations from a point. The tilt derivative uses the arctangent of the first vertical derivative to examine signal amplitudes (Miller and Singh, 1994). This technique examines

the signal amplitudes and centers the anomaly peak about the causative body, rather than at the edges that are typically defined (Jacques et al., 2014).

The analytic signal amplitude removes directions of magnetization to enhance anomaly maximums. The amplitude value from the analytical signal is related to the degree of magnetization of underlying rocks (Macleod et al., 1993; Cooper and Cowan, 2006; Corti, 2011). The high- and low-resolution aeromagnetic datasets were computed separately, then spliced together using Geosoft Oasis montaj™ software (2010) to provide regional magnetic data over Mozambique, without losing the high-resolution magnetic data of Malawi.

Esri software (ArcMap 10) was used, and the zonal geometry for each polyline was manually extracted to plot the frequency of different structural orientations: the bearing and length, and the beginning, middle, and end coordinates. Based on characteristics of the structural provinces, the southern Malawi Rift is divided into different structural domains with distinct orientations.

The same domains that were used to analyze magnetic data form the structural domain boundaries at the surface. These domains are integrated with surface structural maps, with the offset of faults and segmentation of the rift basin, to determine the spatial distribution of strain relationship between pre-existing and modern structural trends. Crustal thickness map from Njinju (2016) was used to investigate relationships between crustal thickness and brittle structure associated with the southern Malawi rift. This map was created using two-dimensional (2D) radially-averaged power spectrum analysis of the World Gravity Model (2012) Bouguer gravity anomalies.

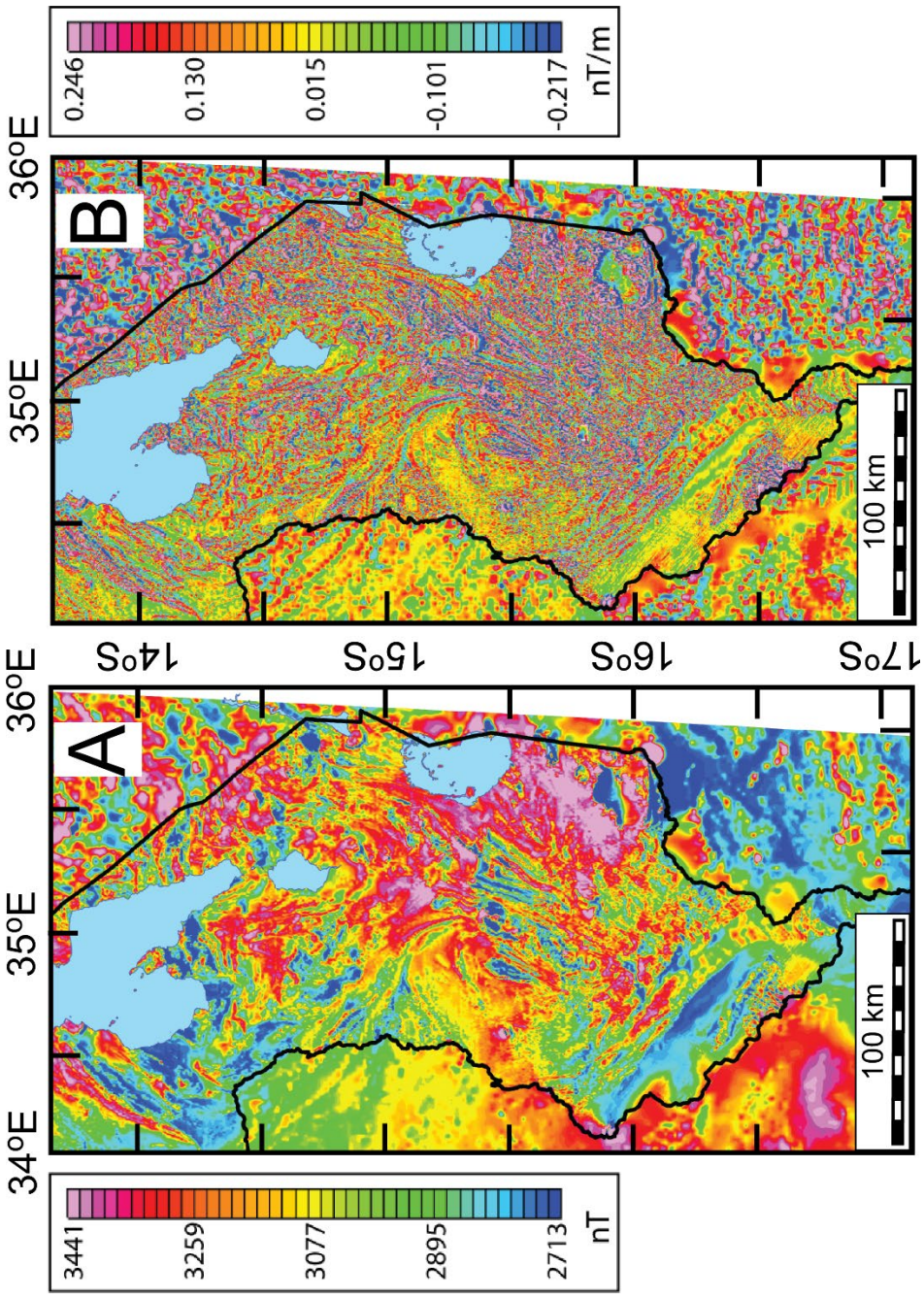

Figure 5: Aeromagnetic data covering the southern Malawi Rift. (A) Total magnetic intensity (TMI) image. (B) First vertical derivative (1VD) image.

CHAPTER IV

RESULTS

4.1 Rift brittle structures

In contrast to the high density of rift brittle structure that are visible in remote sensing images over the rift shoulders and the border faults system of the southern Malawi Rift, the rift floor has few rift brittle structures (Fig. 6). The part that is underlain by the Shire plateau and the Shire Graben south of the southern Malawi Rift also has a lower density of rift brittle structures (Fig. 6).

The rift brittle structures of the southern Malawi rift are divided into six structural domains based on similarity of structural style and orientation (Fig. 7). To relate these structural domains to the evolution of the southern Malawi rift, only the rift brittle structures surrounding the rift with Malawi are considered (Fig. 7). These will be referred to as structural domains 1 – 6 (Fig. 7). The following observations can be drawn: (1) Only domain 4 is characterized by the presence of rift brittle structures that have a uniform NW-SE direction (Fig. 7). This trend dominates the segment of the southern Malawi Rift where it changes orientation from NNW-trending to NE-trending (Fig. 7). The rift brittle structures in this part of the southern Malawi rift are at almost 90^{o} angle to the southeastern border faults system. (2) The rift brittle structures in domains 1 and 6 are characterized by the domination of both NE-SW and NW-SE trends that are perpendicular to each other. In domain 1, the

NW-SE rift brittle structures are sub-parallel to the west-southwestern border faults system of the southern Malawi Rift, while the NE-SW trend of the rift brittle structures in domain 6 coincides with the trend of the southeastern border faults system of the rift (Fig. 7). (3) The orientations of rift brittle structures in domains 2 also have NE-SW and NW-SE oriented trends, as well as an additional NNE trend that is similar to the basement structural frequency data. The data from domain 3 shows a predominantly NW-SE trend and a secondary NE-SE trend that are approximately 75° from each other (Fig. 7). In both domains, the NW-SE trend is sub-parallel to the east-northeastern and west-southwestern border faults system of the southern Malawi Rift. (4) The rift brittle structures in domain 5 do not have any well-defined structural trend (Fig. 7). Rather, the rift brittle structures define an array of structural orientations spreading between NE-SW and NW-SE. Structural domain 6 is within the part of the southern Malawi Rift where the western margin of the rift is defined by three overlapping N-trending and relatively poorly-defined border faults (Fig. 6).

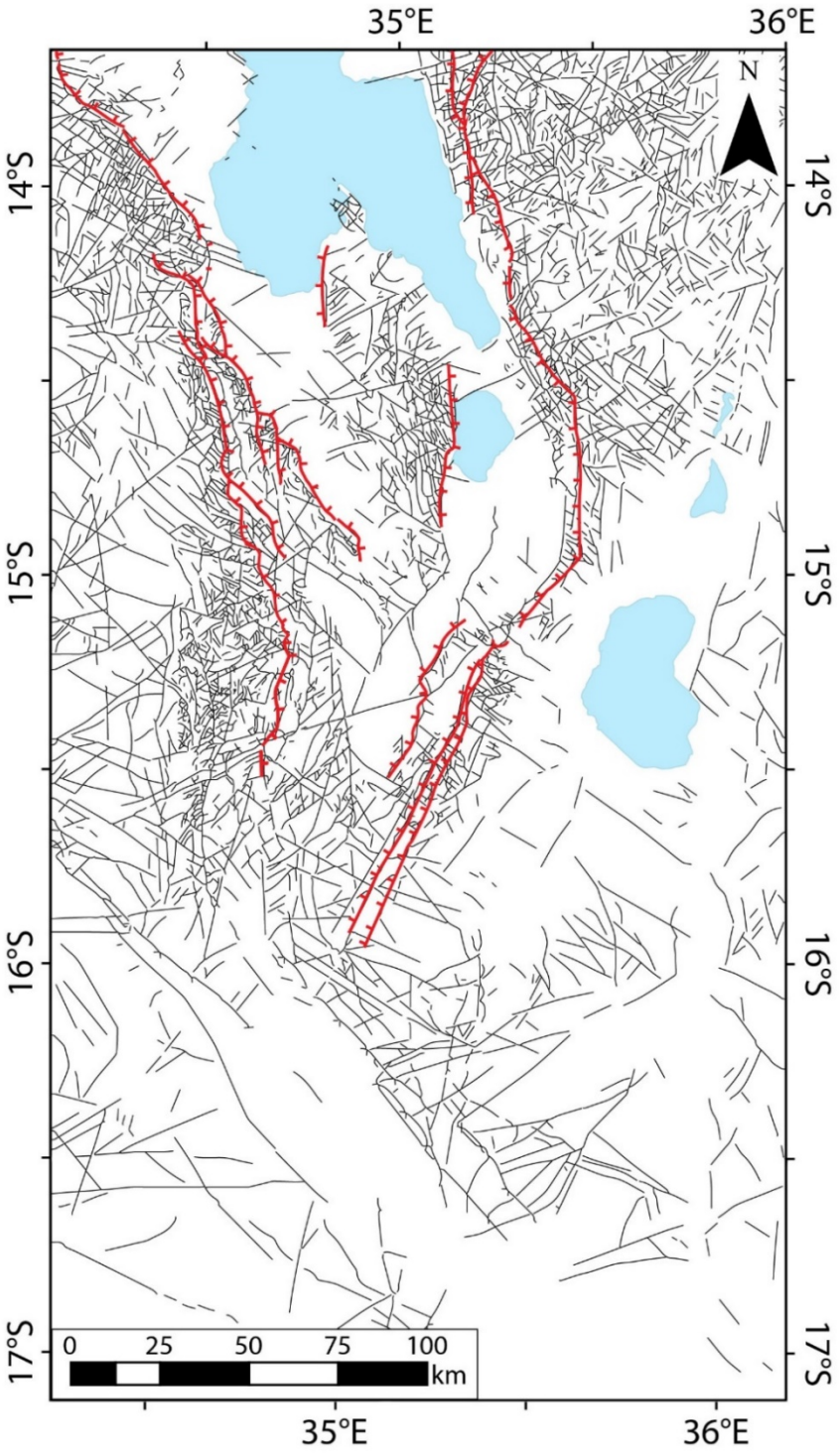

Figure 6: Lineations associated with the southern Malawi Rift structures extracted from the interpretation of the Shuttle Radar Topography Mission (SRTM) Digital Elevation Model (DEM) that is enhanced by color-coded hillshade and horizontal derivative in the y-direction (Dy) as well as the interpretation of the RADARSAT-1 data. The red lines represent the border faults in the southern Malawi Rift Zone.

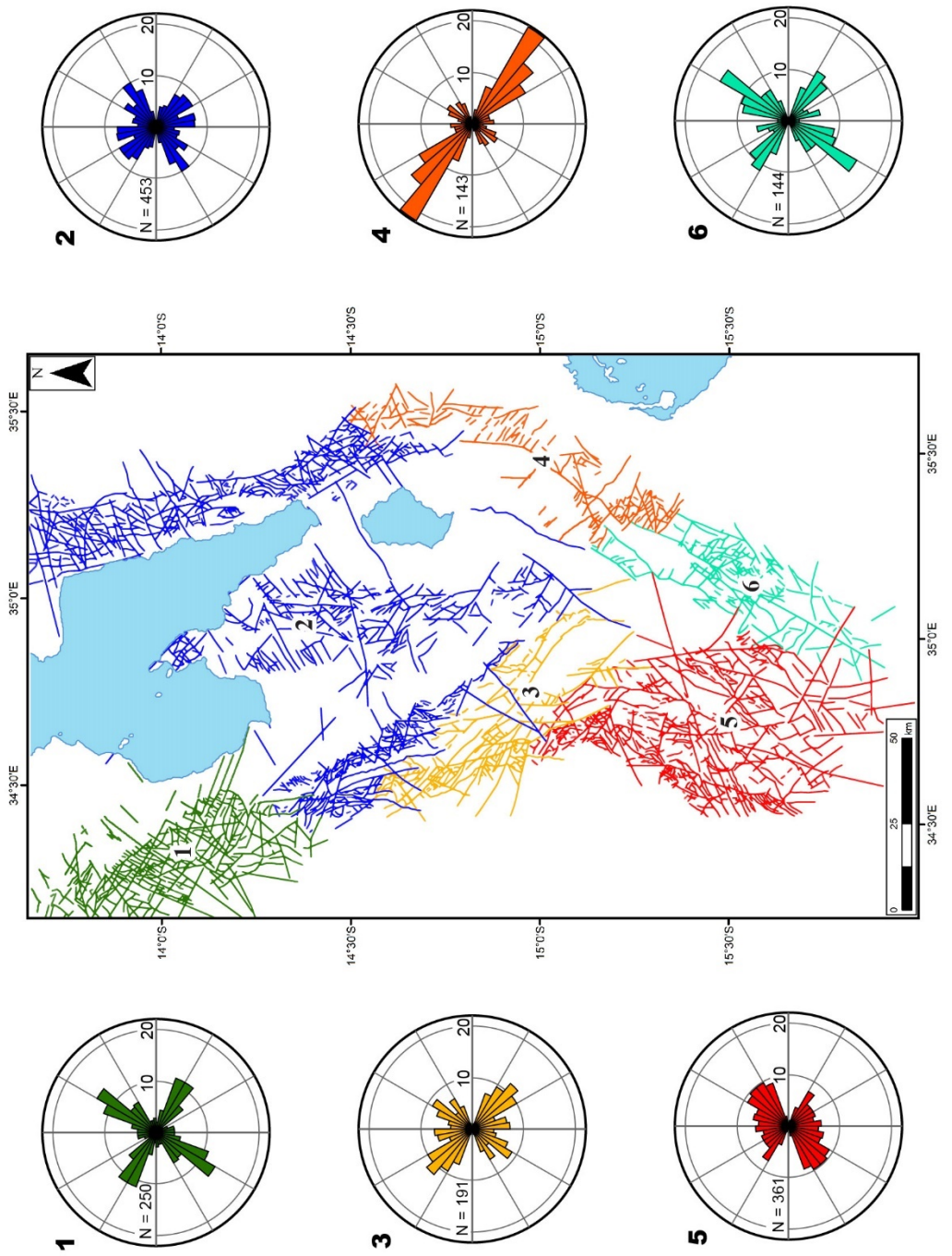

Figure 7: Structural domains of the brittle structure associated with the southern Malawi rift and the rose diagram of each domain.

4.2 Precambrian ductile structures

Different from the rift brittle structures, the Precambrian ductile structures are apparent around the southern Malawi rift and within its floor, except within the Shire Graben (Fig. 8). This is possibly because the Shire Graben is filled with middle Permian to middle Jurassic sedimentary rocks that prevented the aeromagnetic data from imaging the Precambrian ductile structures. The Precambrian ductile structures are divided into six structural domains following the geographic extent of the structural domains established of the rift brittle structures. The following observations can be dawn: (1) The Precambrian ductile structures in domain 1 have a well-defined NE-SW trend that is almost at 90^{o} angle to the west-southwestern border faults system of the southern Malawi Rift (Fig. 9). (2) The Precambrian ductile structures in domain 3 define a NW-SE trend and that this trend is sub-parallel to the west-southwestern border faults of the southern Malawi Rift (Fig. 9). (3) The Precambrian ductile structures in domain 6 define a NNE-SSW trend and that this trend is sub-parallel to the southeastern border faults system of the southern Malawi Rift. (5) Although not well-defined, the Precambrian ductile structures in domain 2 show general NNW-SSE trend and that this trend is sub-parallel to the east-northeastern border fault of the southern Malawi Rift (Fig. 9). The Precambrian ductile structures in domains 4 and 5 define an array of different trends fluctuating between NE-SW and NW-SE (Fig. 9).

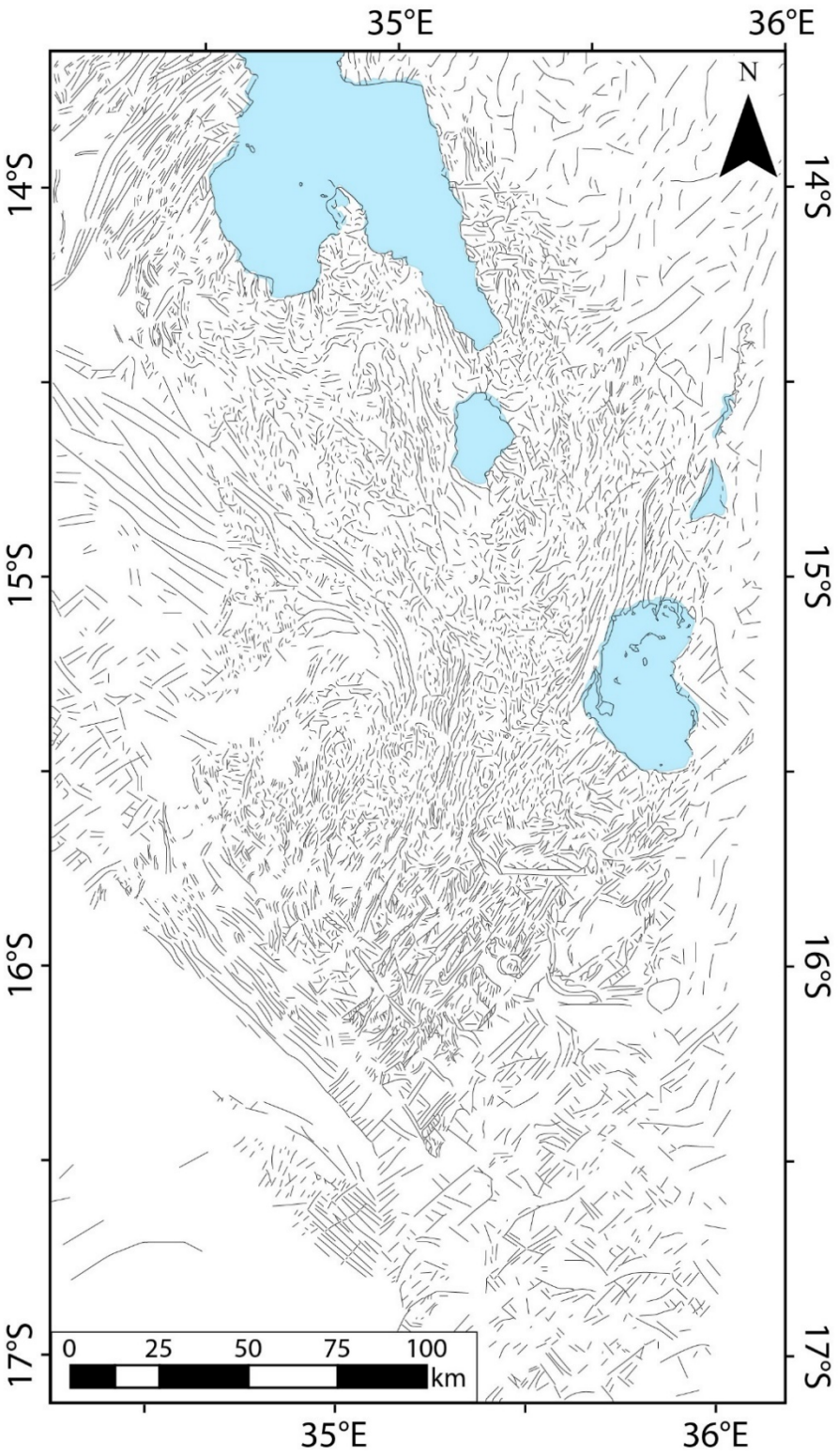

Figure 8: Ductile structure of the Precambrian crystalline basement surrounding the southern Malawi Rift extracted from the interpretation of the first vertical derivative (1VD) of the aeromagnetic data.

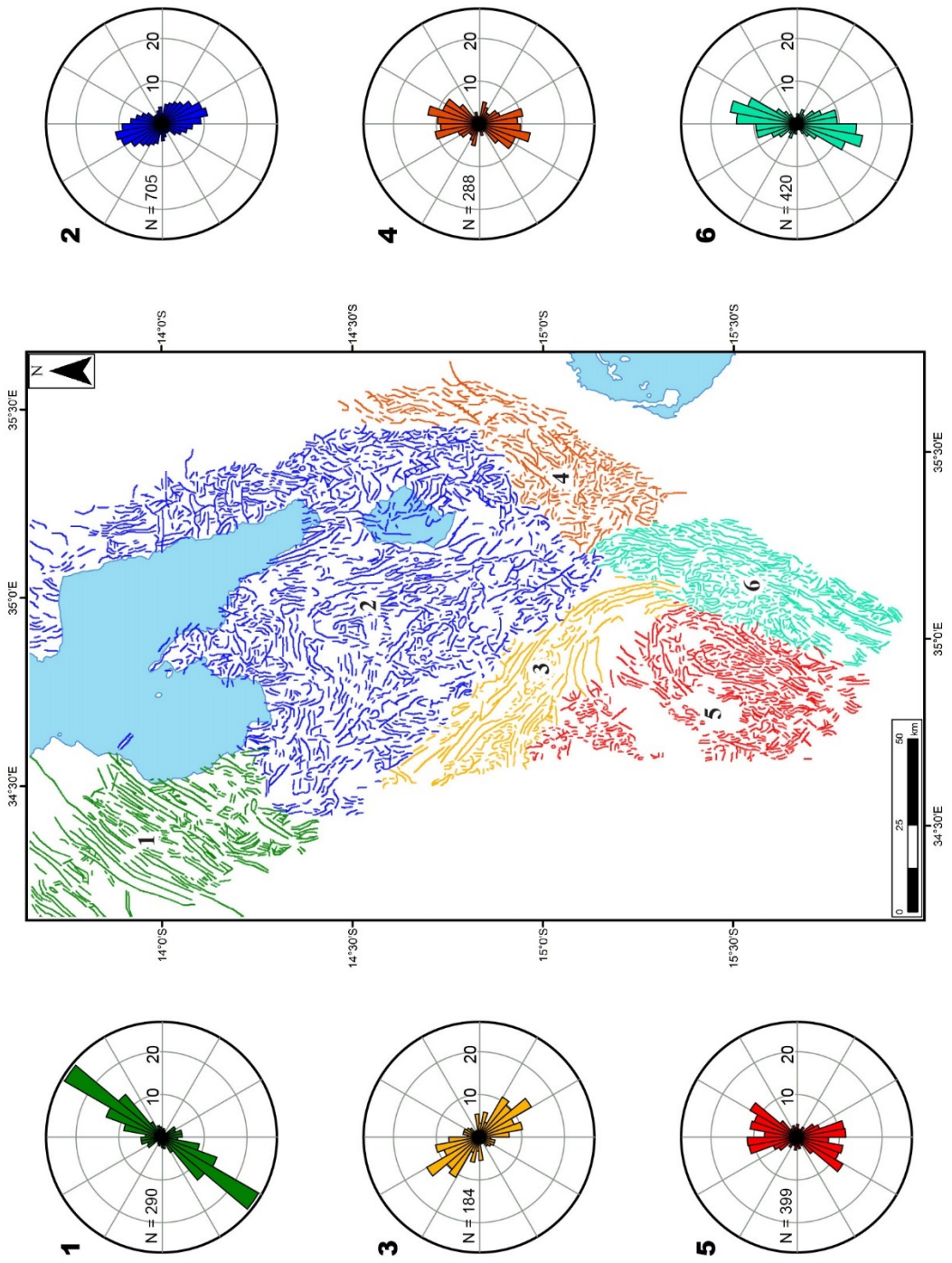

Figure 9: Structural domains of the ductile structure of the Precambrian crystalline basement surrounding the southern Malawi Rift and the rose diagram of each domain.

4.3 Crustal thickness

Figure 10 shows the depth to the Moho beneath the southern Malawi Rift obtained by Njinju et al. (2019) using the two-dimensional radially-averaged power spectral analysis of the World Gravity Model 2012 (WGM 2012).

The crustal thickness in the southern Malawi Rift varies between 35 km and 45 km (Fig. 10). Generally, the thinnest crust is observed in the eastern side of the southern Malawi Rift beneath the Shire plateau. In this region, a crust as thin as 35 km has been observed in the southeastern side of the southern Malawi (Fig. 10). Another region of crustal thinning is found in the north beneath the segment of the southern Malawi Rift that is NNW-trending and is bifurcated by the Shire Graben (Fig. 10). Generally, the western part of the southern Malawi Rift is characterized by the presence of thicker crust that has been interpreted as the result of mafic magmatic under-platting accreted during the Cretaceous in association with the emplacement of the Chilwa Alkaline Province (Nyalugwe et al., 2019).

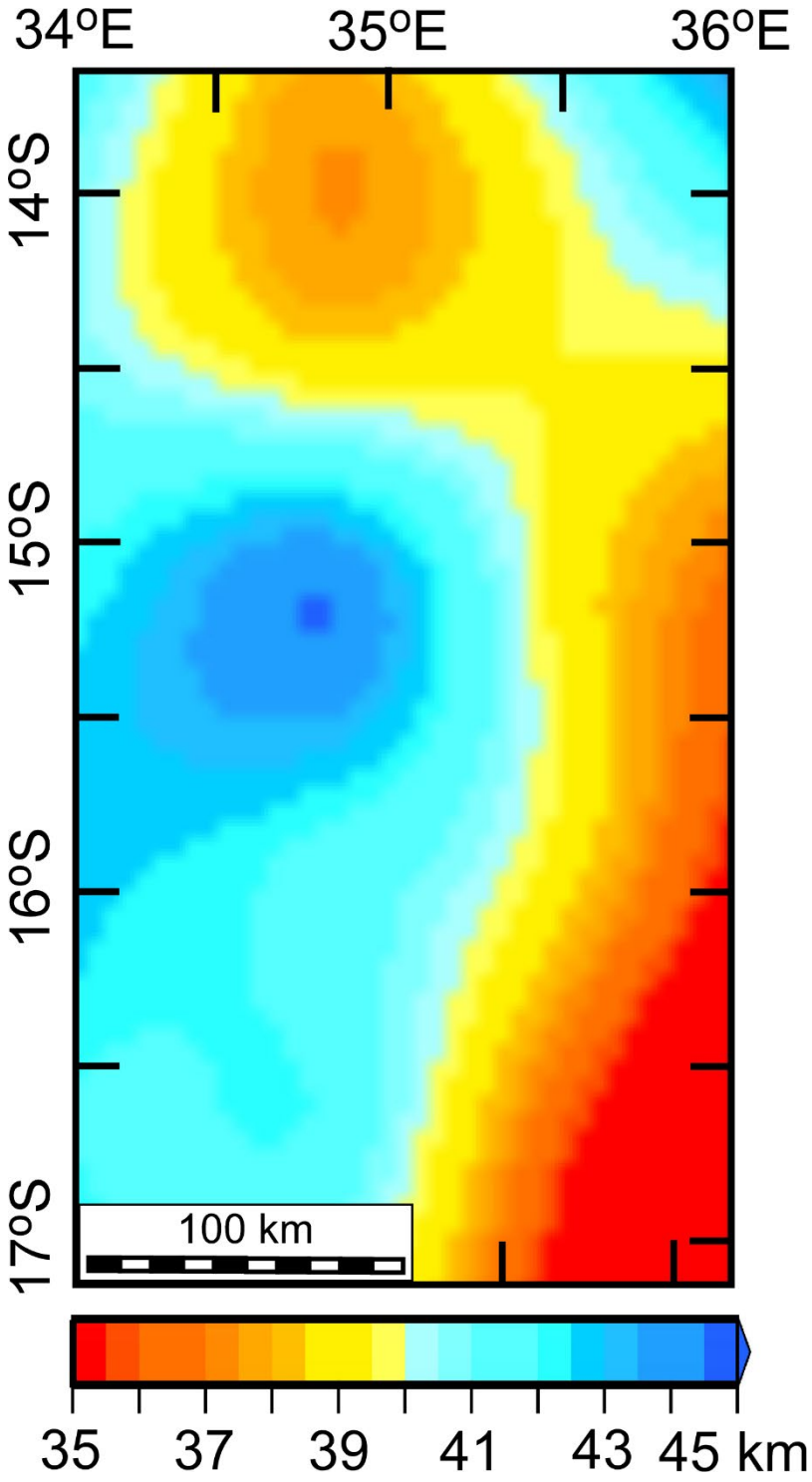

Figure 10: Crustal thickness map of the southern Malawi Rift obtained from the two-dimensional (2D) radially-averaged power spectral analysis of the World Gravity Model 2012 (WGM 2012). After Njinju et al. (2019).

CHAPTER V

DISCUSSION

5.1 The relationship between Cenozoic rift brittle structures and Precambrian ductile structures in southern Malawi

The Precambrian crystalline basement of the southern Malawi Rift is heterogeneous with evidence of several episodes of deformation leaving tectonic scars and large-scale structural grain in basement rock (Fig. 2B; Castaing, 1991; Wilson, 2006; Fagereng, 2013; Fritz et al., 2013; Laó-Dávila et al., 2015; Heron et al., 2016; Peace et al., 2018; Heron et al., 2019). The control of preexisting structures and ductile basement fabrics on the formation of Cenozoic rift brittle structures is one of several, well-documented factors that determine how a rift propagates and influences rifting to different extents in each structural domain (Fig. 7, 9, and 11), creating intricate fault patterns, oblique structures within individual rift segments and deformation segmenting, including basement compartmentalization (Morley, 1990; Wilson, 2006; Agostini et al., 2009; Philips et al., 2016; Fazlikhani et al., 2017). These heterogeneities within the lithosphere create variations in mechanical strength that when favorably oriented, can be inherited by later rift deformation (Peacock and Sanderson, 1992; Morley et al., 2004; Wilson, 2006; Corti et al., 2007; Corti, 2012; Misra and Mukherjee, 2015; Peace et al., 2018; Samsu et al., 2020). Inheritance of brittle structures within the rift shoulders are inconsistent along the

rift-axis; however, examining the interactions of structures within individual domains may contribute to understanding which factors influence the mechanical strength of the crust and most facilitate rift propagation (Samsu et al., 2020).

While the brittle surface structures may indicate directions of extension, cross-cutting relations, and other important rift geometric properties, the current kinematic models cannot account for certain structural interactions, including sudden changes in rift direction, the cross-cutting of strong basement anisotropies and thick crust, or when structures unrelated to far-field stress form separate to rift development, often forming along preexisting structures (Philips et al., 2016; Samsu et al., 2020). For a brittle structure to form along (or reactivate) a preexisting weakness, several factors must be considered. The two factors that seem to influence inheritance in southern Malawi are (1) the strength contrasts in the crust and (2) a favorable orientation between the existing structure or strongly foliated fabric and the local stress direction (Morley, 1999; Cortés et al., 2003; Wilson, 2006; Henza, et al., 2010; Henza, et al., 2011; Misra and Mukherjee, 2015). When the angle between the orientation of basement anisotropy and the ideal trend of new fractures is between 15-45°, fractures are likely to develop parallel the anisotropy or reactivate an existing structure, or form side-stepping, en echelon arrays (Morley, 1999; Corti et al., 2007; Agostini et al., 2009; Samsa et al., 2020); however, when the angle is more than 45°, inheritance does not seem to play a significant role in the development of brittle rift structures (Wilson, 2006; Corti et al., 2007; Aanyu and Koehn, 2011; Misra and Mukherjee, 2015). Figures 7 and 9 support this generalization with frequency data collected in domains 1 and 3 that indicate inheritance is taking place during rifting (Fig. 11). In these domains, one set of brittle structures follows preexisting basement structures in a well-constrained trend and a second set of brittle structures formed nearly perpendicular to the inherited trend. In domain 2, three trends are

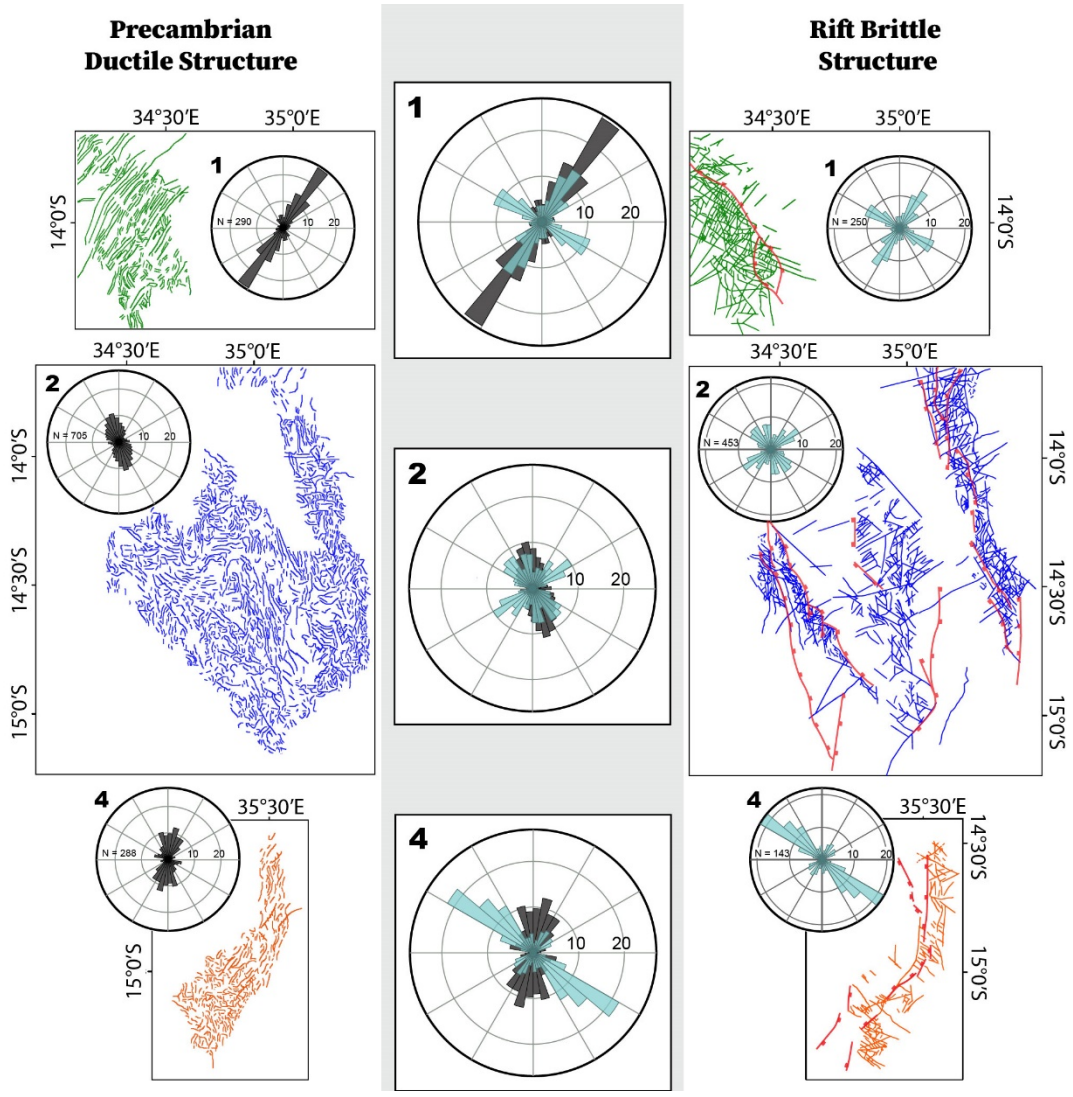

Figure 11: Comparison of structural behavior in Precambrian ductile and rift brittle structures

present in the frequency plots: a NNW-SSE trend subparallel to the tightly constrained basement structures, a NE-SW trend, and a perpendicular NW-SE trend (Fig. 7 and 11). While there is a trend in domain 2 that may have been inherited, the NW-SE trend formed less than 30° from the basement structural trend rather than reactivating or inheriting the NNE-SSW orientation. This could be the due to secondary faulting during later tectonic episodes or by linking existing NNW-SSE oriented fault structures. Like in domain 2, frequency data collected in domains 4, 5, and 6 do not support the presence of inheritance; although, in domain 6, the magnetic anomaly

maps indicate inheritance may have occurred along some NE-trending, strongly foliated gneissic basement structures that are poorly represented in the frequency plots. As shown in Figure 11, the brittle structures react to pre-existing weaknesses in the ductile basement fabric in three ways: 1) inherit the orientation of the basement anisotropies; 2) no correlation; or 3) have at least one trend that inherits the orientation of basement anisotropies and one or more trends that show no correlation.

5.1.1 Southern Malawi Rift border faults

The border fault system in the study area comprises several border fault segments: the western Bilila-Mtakataka, the southwestern Chirobwe-Ncheu, the eastern Mwanjage, the southeastern Zomba, and the southeastern and northwestern Shire Horst border faults (Fig. 12A; Laó-Dávila et al., 2015; Wedmore et al., 2020). In general, the southern Malawi border faults are more diffused than their northern counterparts and often comprise overlapping segments or deformation distributed across multiple interior faults (Fig. 12A and B; Flannery and Rosendahl, 1990; Hori and Tomita, 1997; Corti et al. 2013; Wedmore et al., 2020). Examining the controls on border fault propagation within the study is made more complicated by the overprinting of secondary faulting, en echelon arrays and linking border faults, strongly foliated basement, and Mesozoic intrusions west of Lake Chilwa. There is little elevation change across the southern portion of the Malawi Rift and little sediment-related subsidence in the rift interior. This could result from strain accommodated across interior and exterior faults or approaching the termination of the main rift against the Shire Graben (Fig. 12A and B; Corti et al., 2013; Laó-Dávila et al., 2015).

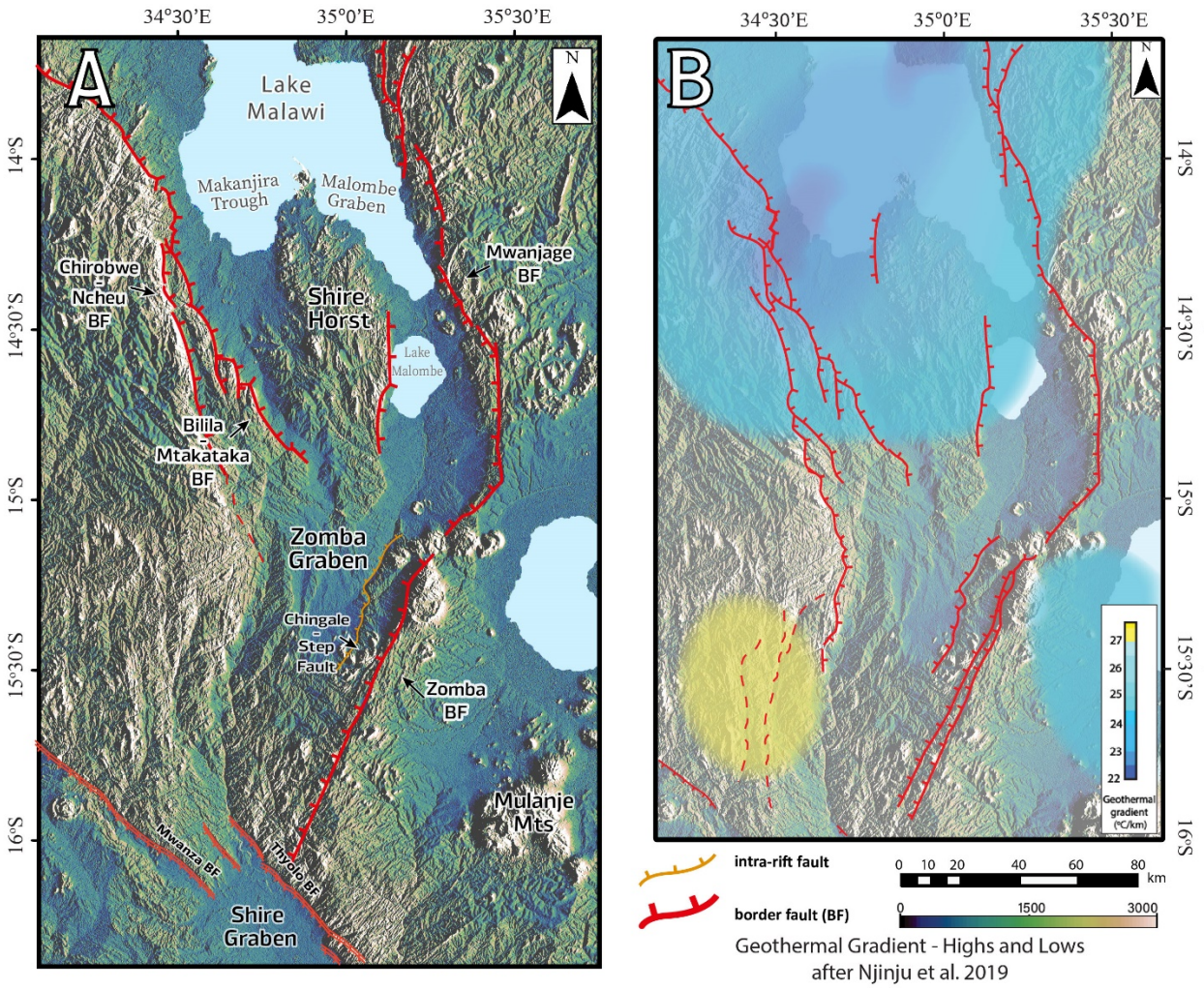

Figure 12: A) Shuttle Radar Topography Mission (SRTM) Digital Elevation Model (DEM) of the southern Malawi Rift with border faults (BF) and major features labelled. (B) Shuttle Radar Topography Mission (SRTM) Digital Elevation Model (DEM) of the southern Malawi Rift with minimum-maximum geothermal gradient after Njinju et al. (2019).

The SRTM and RADARSAT images over the Bilila-Mtakataka border faults indicate the faults were likely a SW-stepping en echelon array linking NNE-SSW oriented faults to form a NW-SE oriented, nearly continuous scarp interior to the Chirobwe-Ncheu border fault (Jackson and Blenkinsop, 1997; Hodge et al., 2018). The brittle structures along the Bilila-Mtakataka fault show the three structural orientations represented in the structural frequency plot of domain 2 (Fig 7 and 11) and similar processes may have occurred on a smaller scale. This finding is in

agreement with research by Hodge et al. (2018), where measured scarp heights along the Bilila-Mtakataka faults show two bell-shaped curves along the middle of the 110 km long fault segments that indicate the Bilila-Mtakataka fault began as independent faults and were hard linked by secondary faults that activated during subsequent tectonic events and rifting.

The exterior Chirobwe-Ncheu border fault formed subparallel to the southern Malawi Rift axis and the basement ductile structures, which indicates inheritance could have contributed to the localization of the fault (Fig. 13). After the Chirobwe-Ncheu border fault diverges from the Bilila-Mtakataka border fault, it can be traced through domain 2, inheriting the same NNE-SSW trend as the basement structures. As the border fault propagated towards the Shire Horst through the Kirk Range in domains 3 and 5, it becomes a series of distributed faults without a continuous scarp, overlapping inheriting the NNE-SSW or NNW-SSE orientations of the basement structures (Fig., 13; Hori and Tomita, 1997). While the Chirobwe-Ncheu border fault tends to inherit structure, the rest of the rift brittle structures in the western rift shoulders show less of a tendency. The variable nature of rift brittle structures along the border faults and the likelihood for inheritance to occur is exemplified in the frequency plots for domains 1, 3, and 5. In domain 1, the brittle structures have well-constrained trendlines that become less constrained in domain 3 and are poorly-constrained in domain 5, varying in structural orientations from NW- to NE-trending (Fig. 7, 9, 12A)

East of the Malombe Graben, the Mwanjage border fault segment strikes NNW-SSE (Fig. 12A and 13). Like many of the border faults in southern Malawi, the fault is not one continuous scarp, but rather a series of normal faults that accommodate strain across them, displacing river channels (Dulanya et al., 2017) and likely interacting with the ductile structure seen in the aeromagnetic data at depth. The faults to either side along-strike the rift of the Shire Horst

distribute strain across several faults, creating splays and the linked en echelon array of the Bilila-Mtakataka fault. At the southern terminus of the Shire Horst, the Mwanjage border fault approaches the Zomba Plateau and Chilwa Alkaline Province (CAP) where the rift axis abruptly changes from NNW- to NNE-striking as the Mwanjage and Zomba border faults link (Fig. 12A). The "kink" formed in the eastern border faults of the study area is 120° and coincides with the Mwanjage border fault encountering NE-striking, strongly foliated gneissic basement structures during propagation that is subsequently inherited by the Zomba border fault (Fig. 13).

Despite the densely clustered Stormberg dikes and suitably oriented structures in the basement fabric, the Zomba border faults grow increasingly diffused along-strike the rift axis through structural domains 5 and 6, with much of the faulting occurring as intra-basin faults in the Zomba Graben (Fig. 12A). The border faults show little vertical displacement and are difficult to distinguish in remote sensing images. The western side of the Shire Graben encompasses the Kirk Range and shows similar features in the diffused border fault system, making distinguishing border faults from remote sensing difficult. Field work by Hori and Tomita (1997) in the Kirk Range recorded similar diffused, overlapping faults as another field study conducted by Wedmore et al. (2020) within the Zomba Graben and discovered that strain accommodation took place across several intra-rift faults instead of the main border faults that usually account for a large percentage of the strain. This supports the frequency plots of structural orientations, which are very diffused in this region and many of the intra-rift features are covered with sediment from Lake Malawi. This area of densely populated rift brittle structures corresponds to the Lower Zomba Graben (Fig 7) and has many laterally extensive joints, fractures, and strong foliations which influence local geomorphology seen through displacement of river channels and remote sensing imagery (Morley, 1995). After nearly 200

kilometers of diffused border faults, the surface expression of the Malawi Rift terminates against the unfavorably-oriented Shire Graben, a NW-striking Karoo basin, oriented nearly 90° from the NNE trajectories of both the southwestern and southeastern border fault systems.

5.2 Rift localization, segmentation, and strain accommodation within the study area

In southern Malawi, the rift propagates through several tectonic terranes, making the relationship between rift localization, geometry, and pre-rift structures difficult to decipher. The lack of evidence for magma-assisted rifting, combined with the diffused border faults, lack of basin subsidence, and incongruous interactions with ductile basement structures mean the driving forces for the southern Malawi Rift propagation remain poorly-understood. Southern Malawi used to be considered the southern continuum of the Irumide Belt, but a terrane subdivision proposed by Johnson et al. (2006) based on geochronological data from Mapani et al. (2001; 2004) verified a tectonically separate belt that formed during the Irumide Orogeny as a result of lithospheric collision during subduction events, the Southern Irumide Belt (SIB). Sarafian et al. (2018) interprets a large, Mesoproterozoic suture in their electrical conductivity model, representing the Mwembeshi Shear Zone, which separates the Irumide and Southern Irumide Belts. Other studies indicate the presence of strong lithosphere across southern Malawi and smaller shear structures, which may hinder the southward propagation of the Malawi Rift (O'Donnell et al., 2013; Adams et al., 2018; Sarafian et al., 2018; Nyalugwe et al., 2019; Celli et al. 2020).

Mulibo and Nyblade (2016) examine seismicity along the East African Rift System, including the central and southern Malawi Rift. The seismic data reveal an abrupt change in seismic behavior near the Mwembeshi Shear Zone that separates the Irumide Belt and the

southern Irumide Belt, north of the study area. Seismic activity markers north of the shear zone representing earthquakes of magnitude 2.5 to 6.5 are densely populated along the border faults. South of the shear zone, the seismic markers are relatively sparse with some markers on either side of the Shire Horst bifurcation, along the border faults west of the Shire Horst and to the southeast of the horst where the BFS abruptly changes from NNW to NE-trending. This change is particularly evident examining the eastern border faults across the shear zone as the Metangula border fault segment north of the study area experiences large amounts of activity and the Mwanjage and Zomba border faults experience a much lower frequency of seismic activity. While the Bilila-Mtakataka border fault is known for being seismically active (Jackson and Blenkinsop, 1997; Hodge et al., 2018), the events are far less common when compared to the seismic activity in the northern Malawi Rift. The change in seismic behavior is an indicator of heterogeneous mechanical strength within the lithosphere and supports the presence of strong lithosphere across the southern Malawi Rift.

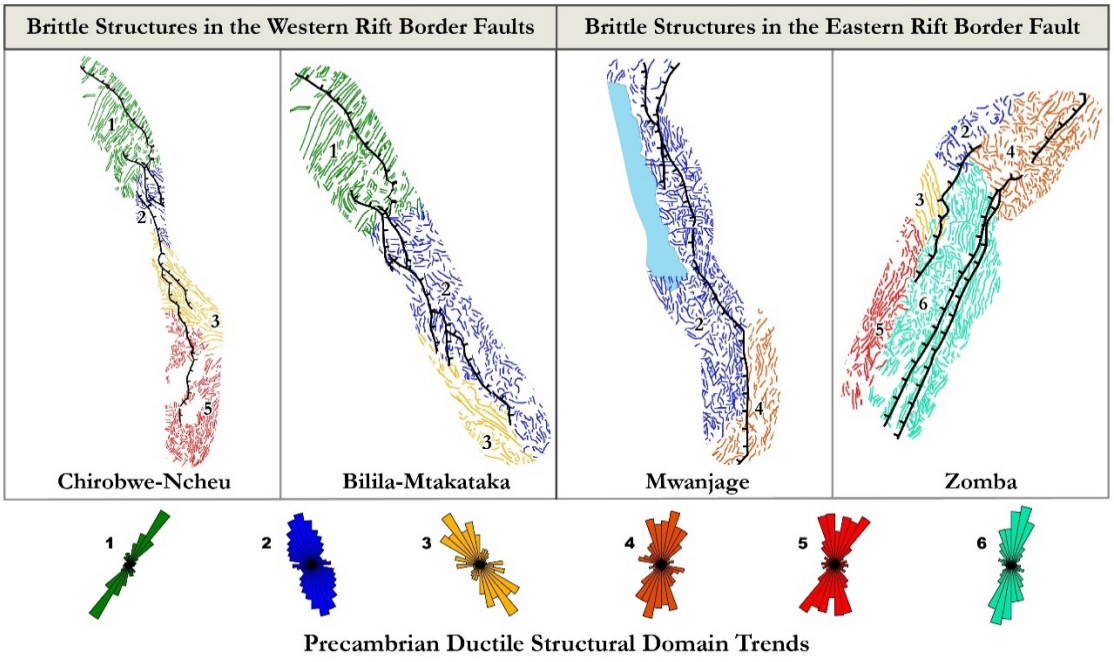

Figure 13: Structural frequency domains corresponding to the Chirobwe-Ncheu, Bilila-Mtakataka, Mwanjage, and Zomba border faults.

5.2.1 Malawi Rift bifurcation around the Shire Horst

One of the most prominent rift features in southern Malawi remains one of the least understood: the rift bifurcation around the Shire Horst (Fig. 12A). Previous research of southern Malawi Rift processes has suggested controlling factors for the divergence around the Shire Horst, which is generally acknowledged to consist of more resistant than the surrounding basement complex, but most studies over the southern Malawi Rift do not put forth any evidence supporting theories on the bifurcation. However, recent studies investigating the lithospheric structure of Malawi, Zambia, and Mozambique provide evidence of strong lithosphere within the study area that may indicate the eastern reaches of the Archean Niassa cratonic nucleus within the Southern Irumide Belt, west of the Shire Horst (Andreoli, 1984; Daly et al., 1989; Piper,

1989; De Waele et al., 2006, 2009; Adams et al., 2018; Sarafian et al., 2018; Njinju et al., 2019; Celli et al., 2020).

The interaction between thick cratons within the lithosphere has long been acknowledged as a primary control for rift localization, e.g. the East African Rift avoids the thick, cool, tectonically stable cratons, preferentially propagating through the margins of orogenic belts and shear zones, skirting stable cratons in a curvilinear manner (Corti et al., 2013). While this interaction is clear on a large scale, the geophysical resolution needed to distinguish similar observations at a rift segment scale is scarce over the study area (Adams et al. 2018; Sarafian et al., 2018). If the "lost" Niassa craton is beneath the thick sedimentary cover overlying the Southern Irumide Belt, it could be responsible for the increased crustal thickness and locally decreased geothermal gradient calculated by Njinju et al. (2019) (Fig. 12B). This would also create a disparity in mechanical strength between the preserved craton and the surrounding lithosphere, which could contribute to rift localization, particularly the sudden change in the rift axis from NNW- to NE-striking, rift segmentation, and the geographic extent of igneous features from events like the Chilwa Alkaline Province (Fig. 12A); Sarafian et al., 2018; Nyalugwe et al., 2019; Celli et al., 2020).

Several recent studies use different geophysical techniques to map the extent of an anomalous structure to the west of the southern Malawi Rift and interpret that anomaly to be the Niassa Craton: Adams et al. (2018) use Rayleigh wave phase velocity tomography and propose the high-velocities across southern Malawi suggest several Archean cratonic roots could be responsible for controlling rift propagation through preexisting strong lithosphere; Sarafian et al. (2018) use electromagnetic lithospheric imaging using the magnetotelluric method to interpret a suture zone between the Bangweulu Block to the north and the northern edge of the Niassa

Craton; Njinju et al. (2019) use 2D radially averaged power spectrum analysis of aeromagnetic data to examine the thermal structure beneath the Malawi Rift and found a low-thermal signature indicative of cratonic lithosphere over the Shire Horst region of Malawi, and Celli et al. (2020) use high-resolution tomography to map the geographic extent of the Niassa Cratonic root at depth. Differences in resolution, as well as local heterogeneities in the cratonic crust caused the different techniques to produce different geographic extents for the Niassa Craton. At a depth of 80150 km, a high-resolution tomography model from Celli et al. (2020) established the eastern boundary of the Niassa Cratonic, northeast of the Shire Horst that coincides with the rift bifurcation.

Njinju et al. (2019) used Curie Point Depths (CPD) to model thermal structures across the Malawi Rift and found a band of anomalous low-gradient heat dispersion across the Shire Horst. This area has a substantially lower gradient than the rest of the rift interior. The presence of the low-gradient in geothermal energy makes magmatism an unlikely driving force for the rift bifurcation and propagation in this region. This finding is in agreement with data collected by Atekwana et al. (2016), which used gaseous geochemical analysis to determine that samples collected from the Central and South Sections of Malawi hot springs did not have the characteristic chemical signature expected from mantle derived hot springs. From the northern Rungwe Volcanic Province to the Shire Graben, hot springs are a common occurrence along the western rift shoulder, the only exception being the 195 km long distance along the rift axis that corresponds to the region of cool, thick crust near the Shire Horst. The cratonic root (as mapped by Celli et al., 2020) may remain tectonically stable and largely unaltered, but cratonic crusts may be reworked throughout orogenic and rift events. The areas with the lowest geothermal gradient may indicate Archean Niassa cratonic crust not protected by the cratonic nucleus is

being reworked with the Southern Irumide Belt lithosphere and it would be unlikely to produce the heat required for geothermal springs (Fig. 12B).

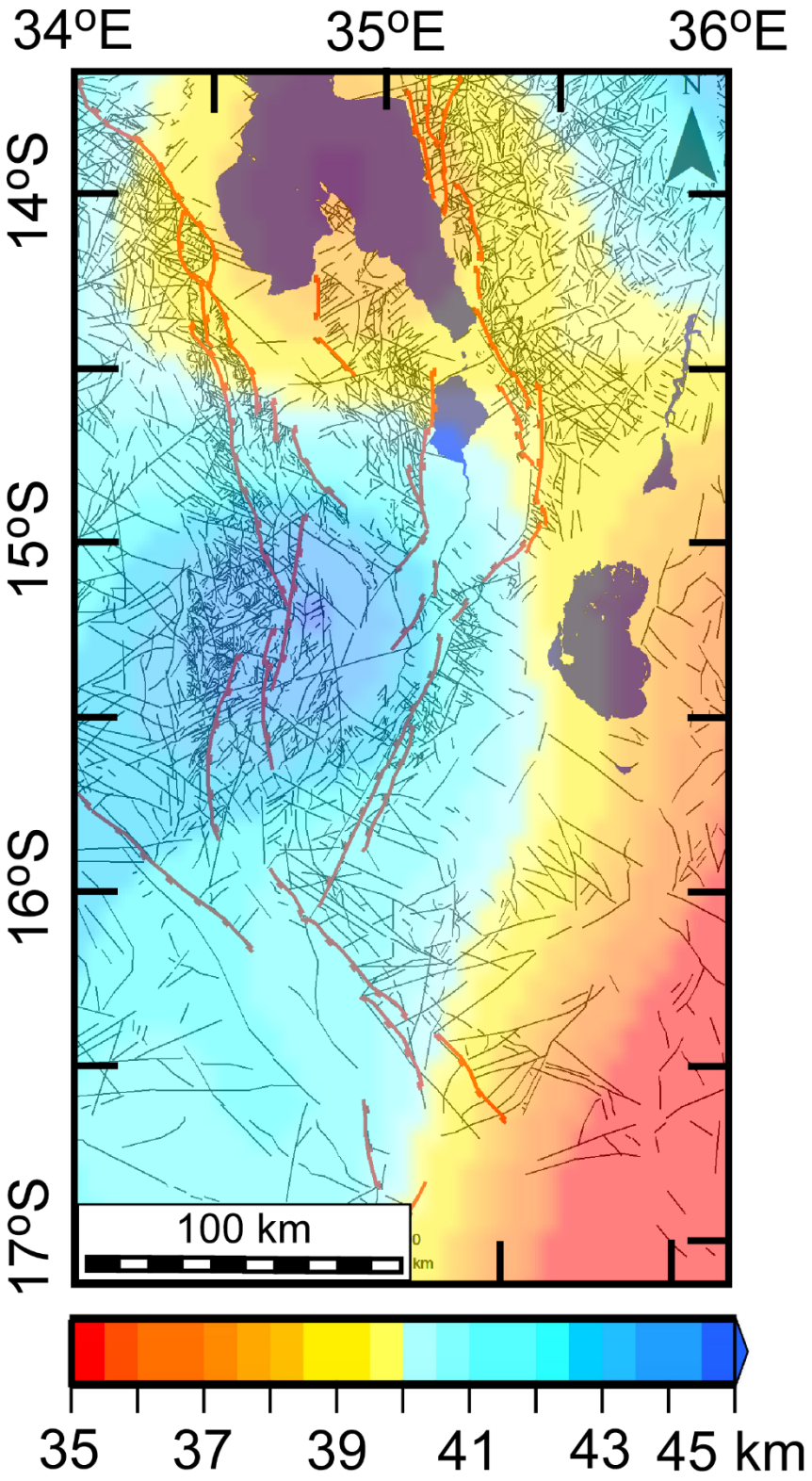

Figure 14: Brittle structure associated with the southern Malawi Rift draped onto the crustal thickness image of Njinju et al. (2019).

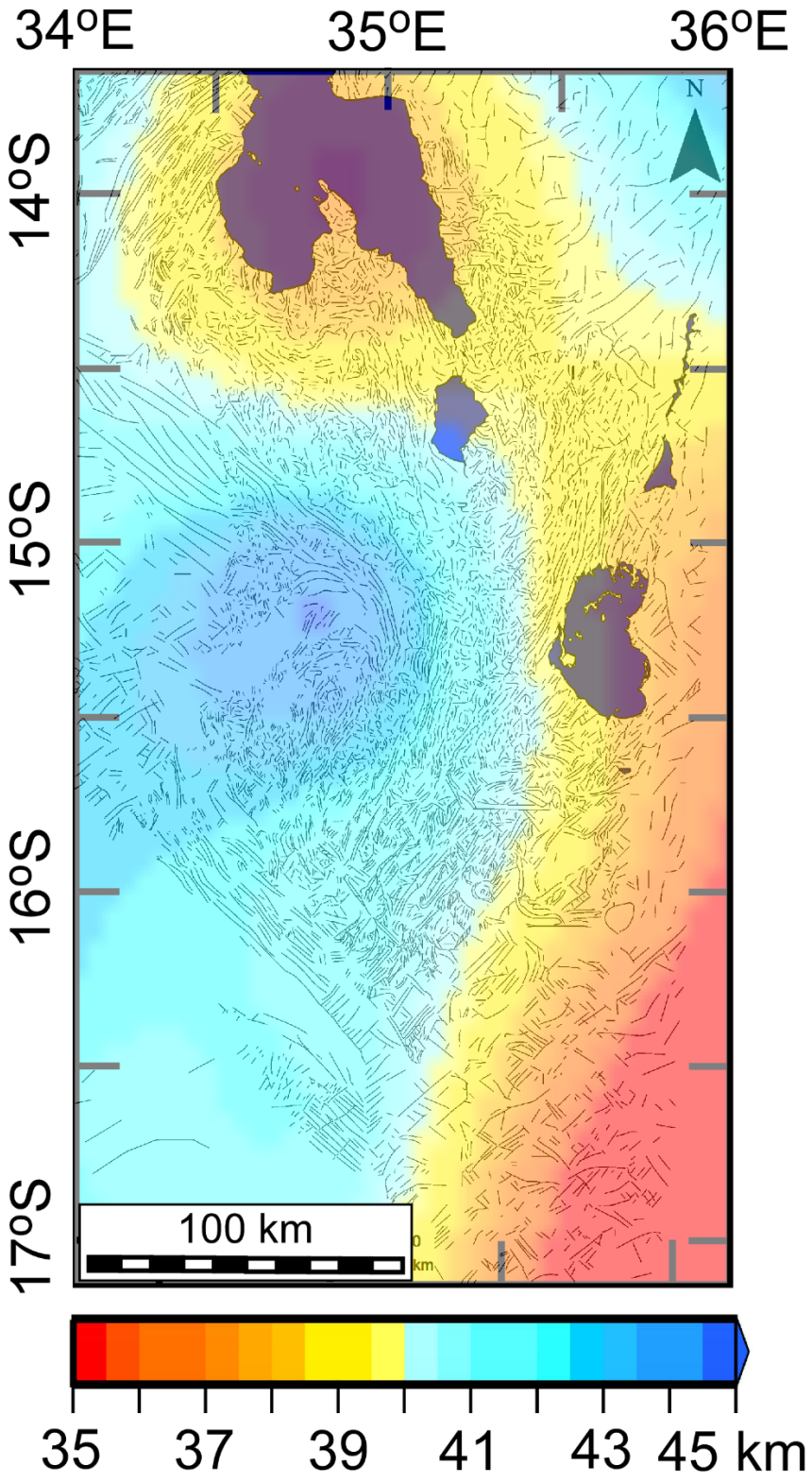

Figure 15: Ductile structure of the Precambrian crystalline basement surrounding the southern Malawi Rift draped onto the crustal thickness image of Njinju et al. (2019).

5.2.2 The Bilila-Mtakataka, Chirobwe-Ncheu, and Mwanjage border fault segments

Rift segmentation is more prominent in the northern Malawi Rift than the southern portion. In the case of the southern Malawi Rift, the Niassa Cratonic root may have controlled the localization of the western rift boundary and influenced the geometry of the rift and the border faults that propagate through the cool, thick lithosphere. In Figure 12B the approximate location of the Niassa Craton area of influence is inferred from deep CPDs (24-27 km) and a low geothermal gradient (Njinju et al., 2019). When superimposed on structural maps over the study area, the thick, cold lithosphere extends under the Shire Horst, marking a change in the geometry of the Malawi Rift (Fig. 12B). The lowest portions of the geothermal gradient coincide with areas with diffuse bounding faults, resulting in splays and bifurcation in the southern Malawi Rift border fault system. The cooler crust located over the Shire Horst, for instance, likely caused the rift bifurcation.

The western and northeastern border faults are located within the low-geothermal anomaly and all except the Bilila-Mtakataka border fault go around the coolest portions of the craton, leaving 2 areas of the lowest-geothermal gradient crust within the rift (Fig. 12B). In Figures 14 and 15, brittle and ductile structures are draped over a crustal thickness image from Njinju et al. (2019). The figures both show relationships with the structures and the crustal thickness data: the foliations of the Precambrian ductile structures correspond in orientation with the margins of the thicker crust and curve around the ~45 km thick crust to the south west of the Shire Horst and the (Fig. 15).

The western border faults propagated along the western margin of the southern anomaly, separating into the Chirobwe-Ncheu and Bilila-Mtakataka border faults. The termination of the

Bilila-Mtakataka border fault segment occurs near the Shire Horst termination and coincides with the southern edge of the cool anomaly (Fig. 12B, 14, 15).

5.2.3 The Zomba border fault segment and intra-rift structures

Mesozoic igneous activity including intrusions from the Chilwa Alkaline Province, Chingale Igneous Ring Complex, Stormberg Dikes, are almost exclusively located within the region of thick lithosphere in the east-southeast of the study area, surrounding a localized ellipse of thick, cool crust that corresponds to a region that has low-levels of deformation, southeast of the Zomba Plateau (Fig. 12A).

While many of the intra-rift structures are covered by sediments deposited by the Shire River and its tributaries, it is possible to deduce significant intra-rift faults from abrupt changes in river geometry (Dulanya et al., 2017). Wedmore et al. (2020), mapped several intra-rift faults in the Zomba Graben, including the well-established Chingale Step fault, near the Zomba border fault, to better understand strain accommodation along the southern rift. They calculated that 55 ± 24 % of extensional strain is accommodated within intrabasin faults across the Zomba Graben. While the error margin for the extensional strain accommodation along the intra-rift structures is large, it still gives more potential for strain accommodation in the rift interior than previously considered (Fig. 12A).

The results of this study suggest inheritance occurs within individual sections of the Malawi Rift or when strongly foliated fabric is favorably oriented; however, the rift axis does not indiscriminately follow basement anisotropy or structures. This leads to the conclusion that another factor, like the presence or the Niassa Craton or changes in lithospheric thermal

properties and thickness, may be a more significant control on rift location and propagation than structural inheritance, which may exert a secondary control on the behavior of rift structures.

CHAPTER VI

CONCLUSIONS

In southern Malawi, Cenozoic rift brittle structures are superimposed on the already complex basement terrain, creating an environment with varying degrees of inheritance of the Precambrian crystalline ductile basement structures. Our research suggests a predisposition for rift brittle structures to inherit ductile basement structures provided the inheritable structure is favorably oriented. In the study area, rift brittle structures react to preexisting structures in three ways: 1) inherit the dominate trend of the basement anisotropies; 2) no correlation; or 3) at least one trend that follows basement anisotropies and one or more trends show no correlation. While inheritance cannot account for many aspects of the southern Malawi Rift, it still plays an important role in the localization and orientation of rift structures, as well as how the rift may accommodate strain, particularly on the border faults and intra-basin faults where many faults experience seismic activity.

Rift segmentation is more prominent in the northern Malawi Rift than the southern portion; however, the unique heterogeneous nature of the lithosphere in the southern Malawi Rift may shed light on the influence of cratonic roots on young continental rift propagation and explain some of the anomalous rift geometries, like the rift bifurcation around the Shire Horst and the abrupt change in orientation along the eastern border fault system. In the case of the

southern Malawi Rift, the Niassa Cratonic root may have controlled how far west the rift propagated and influenced the geometry of the rift and western border faults.

REFERENCES

Adams, A., Miller, J. and Accardo, N., 2018, Relationships between lithospheric structures and rifting in the East African Rift System: A Rayleigh wave tomography study. Geochemistry, Geophysics, Geosystems, 19(10), pp.3793-3810.

Briggs, I.C., 1974, Machine contouring using minimum curvature, *Geophysics, 39*(1).

Bloomfield, K., 1966, 1: 1, 000,000 Geological map of Malawi, *Geological Survey of Malawi.*

Buck, W.R., 2006. The role of magma in the development of the Afro-Arabian Rift System. Geological Society, London, Special Publications, 259(1), pp.43-54.

Calais, E., Ebinger, C., Hartnady, C., and Nocquet, J., 2006, Kinematics of the East African Rift from GPS and earthquake slip vector data, *Geological Society, London, Special Publications, 259*, 9.

Castaing, C., 1991, Post-Pan-African tectonic evolution of South Malawi in relation to the Karroo and recent East African rift systems, *Tectonophysics, 191*(1), 55–73.

Catuneanu, O., Wopfner, H., Eriksson, P. G., Cairncross, B., Rubidge, B. S.., Smith, R. M. H., and Hancox P. J., 2005, The Karoo basins of south-central Africa. *Journal of African Earth Sciences*, *43*(1-3), 211-253.

Celli, N.L., Lebedev, S., Schaeffer, A.J. and Gaina, C., 2020. African cratonic lithosphere carved by mantle plumes. Nature communications, 11(1), pp.1-10.

Chapola, L. S., and Kaphwiyo, C. E., 1992, The Malawi rift: geology, tectonics and seismicity. *Tectonophysics, 209*(1-4), 159-164.

Chorowicz, J, J. Fournier, G. and Vidal, 1987, A model for rift development in Eastern Africa. – *Geological Journal, 22*, Thematic Issue, 495-513.

Chorowicz, J. and Sorlien C., 1992, Oblique extensional tectonics in the Malawi Rift, Africa, *Geological Society of America Bulletin, 104*(8), 1015–1023.

Chorowicz, J., 2005, The East African rift system, *Journal of African Earth Sciences*, *43*(1), 379–410.

Contreras, J., Anders, M.H., and Scholz, C.H., 2000, Growth of a normal fault system: Observations from the Lake Malawi basin of the east African rift, *Journal of Structural Geology, 22*(2), 159–168.

Cooper, G. R. J. and Cowan D. R., 2004, Filtering using variable order vertical derivatives. *Computers & Geosciences, 30*(5), 455-459.

Cooper, G. R. J. and Cowan, D. R., 2006, Enhancing potential field data using filters based on the local phase. *Computers & Geosciences, 32*(10), 1585-1591.

Cooper, G. R. J. and Cowan, D. R., 2011, A generalized derivative operator for potential field data. *Geophysical Prospecting, 59*(1), 188-194.

Corti, G., van Wijk, J., Cloetingh, S., and Morley, C. K., 2007, Tectonic inheritance and continental rift architecture: Numerical and analogue models of the East African Rift system, *Tectonics, 26*(6).

Corti, G., 2012, Evolution and characteristics of continental rifting: Analog modeling-inspired view and comparison with examples from the East African Rift System. *Tectonophysics, 522*, 1-33.

Corti, G., Iandelli, I., and Cerca, M., 2013a, Experimental modeling of rifting at craton margins. *Geosphere; 9*(1), 138–154.

Corti, G., Ranalli, G., Agostini, A., Sokoutis, D., 2013b, Inward migration of faulting during continental rifting: effects of pre-existing lithospheric structure and extension rate, *Tectonophysics 594,* 137–148.

Daly, M., Chorowicz, J., and Fairhead, J., 1989, Rift basin evolution in Africa: the influence of reactivated steep basement shear zones, *Geological Society, London, Special Publications, 44*(1), 309-334.

Delvaux, D., 1989, The Karoo to Recent rifting in the western branch of the East-African Rift System: A bibliographical synthesis. Mus. roy. Afr. centr., Tervuren (Belg.), Dépt. Géol. Min., Rapp. ann, 1990(1991), pp.63-83.

Delvaux, D., 1991, The Karoo to Recent rifting in the western branch of the East-African Rift System. A bibliographical synthesis, *Royal Museum for Central Africa, Department of Geology and Mineralogy, B-3080 Tervuren (Belgium),* 63-83.

Delvaux, D., Levi, K., Kajara, R., and Sarota, J., 1992, Cenozoic paleostress and kinematic evolution of the Rukwa – North Malawi rift valley (East African Rift System). *Bulletin des Centres de Recherche Exploration Production Elf-Aquiaine, 16*(2), 383–406.

Delvaux, D., 2001, Tectonic and palaeostress evolution of the Tanganyika-Rukwa-Malawi rift segment, East African rift System. *Peri-Tethys Memoir*, *6*, 545-567.

Dill, H. G., 2007, A review of mineral resources in Malawi: with special reference to aluminium variation in mineral deposits. *Journal of African Earth Sciences, 47*(3), 153-173.

Dunbar, J. A., and Sawyer, D. S., 1988, Continental rifting at pre-existing lithospheric weaknesses. *Nature, 333*(6172), 450.

Dulanya, Z., 2017, A review of the geomorphotectonic evolution of the south Malawi rift, *Journal of African Earth Sciences, 129*, 728-738.

Ebinger, C. J., Rosendahl, B., and Reynolds, D., 1987, Tectonic model of the Malaŵi rift, Africa, *Tectonophysics, 141*(1), 215–235.

Ebinger, C., Deino, A., Drake, R., and Tesha, A., 1989, Chronology of volcanism and rift basin propagation: Rungwe Volcanic Province, East Africa, *Journal of Geophysical Research: Solid Earth, 94*(B11), 15785-15803.

Ebinger, C., Deino, A., Tesha, A., Becker, T., and Ring, U., 1993, Tectonic controls on rift basin morphology: Evolution of the Northern Malawi (Nyasa) Rift, *Journal of Geophysical Research: Solid Earth, 98*(B10), 17821-17836.

Ebinger, C., 2005, Continental break-up: the East African perspective. Astronomy & Geophysics, 46(2), pp.2-16.

Eby, G. N., Woolley, A. R., Din, V., and Platt, G., 1998, Geochemistry and petrogenesis of nepheline syenites: Kasungu-Chipala, Ilomba, and Ulindi nepheline syenite intrusions, North Nyasa Alkaline Province, *Malawi: Journal of Petrology, 39*(8), 1405-1424.

Fagereng, A., 2013, Fault segmentation, deep rift earthquakes and crustal rheology: Insights from the 2009 Karonga sequence and seismicity in the Rukwa-Malawi zone. *Tectonophysics 601*, 216-225.

Fairhead, J. D. and Stuart, G. W., (1982), The seismicity of the East-African rift system and comparison with other continental rifts. *Continental and Oceanic Rifts, 8*, 41-61.

Fazlikhani, H., Fossen, H., Gawthorpe, R.L., Faleide, J.I. and Bell, R.E., 2017, Basement structure and its influence on the structural configuration of the northern North Sea rift. Tectonics, 36(6), pp.1151-1177.

Flannery, J. and Rosendahl, B., 1990, The seismic stratigraphy of Lake Malawi, Africa: Implications for interpreting geological processes in lacustrine rifts, *Journal of African Earth Sciences*, *10*(3), 519–548.

Fritz, H., Abdelsalam, M. G., Ali, K., Bingen, B., Collins, A., Fowler, W., Ghebreab, C., Hauzenberger, P., Johnson, and T. Kusky, 2013, Orogen styles in the East African Orogen: A review of the Neoproterozoic to Cambrian tectonic evolution, *Journal of African Earth Sciences, 86*, 65–106.

Ganiyu, S. A., Badmus, B. S., Awoyemi, M. O., Akinyemi, O. D., and Olurin, O. T., 2013, Upward continuation and reduction to pole process on aeromagnetic data of Ibadan Area, South-Western Nigeria, *Earth Science Research, 2*(1), 66.

Heilman, E., Kolawole, F., Atekwana, E.A. and Mayle, M., 2019, Controls of basement fabric on the linkage of rift segments. Tectonics, 38(4), pp.1337-1366.

Heron, P.J., Pysklywec, R.N. and Stephenson, R., 2016, Identifying mantle lithosphere inheritance in controlling intraplate orogenesis. Journal of Geophysical Research: Solid Earth, 121(9), pp.6966-6987.

Hodge, M., Biggs, J., Fagereng, Å., Elliott, A., Mdala, H. and Mphepo, F., 2019, A semi-automated algorithm to quantify scarp morphology (SPARTA): application to normal faults in southern Malawi. Solid Earth, 10(1), pp.27-57.

Hodge, M., Fagereng, Å., Biggs, J. and Mdala, H., 2018, Controls on early-rift geometry: New perspectives from the Bilila-Mtakataka Fault, Malawi. Geophysical Research Letters, 45(9), pp.3896-3905.

Hori and Tomita (鹿児島大学理学部紀要), 1997, Regional Geochemical Reconnaissance of Kirk Range-Lisungwe, Malawi.

Jepson, A., 2005, 2D Fourier Transforms. *Personal Collection of A. Jepson, University of Toronto, Canada.*

Johnson, S.P., De Waele, B. and Liyungu, K.A., 2006, U-Pb sensitive high-resolution ion microprobe (SHRIMP) zircon geochronology of granitoid rocks in eastern Zambia: Terrane subdivision of the Mesoproterozoic Southern Irumide Belt. Tectonics, 25(6).

Katumwehe, A.B., Abdelsalam, M.G. and Atekwana, E.A., 2015, The role of pre-existing Precambrian structures in rift evolution: The Albertine and Rhino grabens, Uganda. Tectonophysics, 646, pp.117-129.

Kendall, J.M., Stuart, G.W., Ebinger, C.J., Bastow, I.D. and Keir, D., 2005, Magma-assisted rifting in Ethiopia. Nature, 433(7022), pp.146-148.

Koptev, A., Calais, E., Burov, E., Leroy, S. and Gerya, T., 2015, Dual continental rift systems generated by plume–lithosphere interaction. Nature Geoscience, 8(5), pp.388-392.

Koptev, A., Gerya, T., Calais, E., Leroy, S. and Burov, E., 2018, Afar triple junction triggered by plume-assisted bi-directional continental break-up. Scientific reports, 8(1), pp.1-7.

Kreuser, T., 1995, Rift to drift evolution in Permian-Jurassic basins of East Africa. *Geological Society, London, Special Publications*, *80*(1), 297-315.

Laó-Dávila, D. A., Al-Salmi, H. S., Abdelsalam, M. G., and Atekwana, E. A., 2015, Hierarchical segmentation of the Malawi Rift: The influence of inherited lithospheric heterogeneity and kinematics in the evolution of continental rifts, *Tectonics, 34*(12), 2399-241.

Lehar, S., 1999, Gestalt isomorphism and the quantification of spatial perception. *Gestalt theory*, *21*, 122-139.

Leseane, K., Atekwana, E. A., Mickus, K. L., Abdelsalam, M. G., Shemang, E. M., and Atekwana, E. A., 2015, Thermal perturbations beneath the incipient Okavango Rift Zone, northwest Botswana*, Journal of Geophysical Research: Solid Earth, 120*(2), 1210-1228.

MacLeod, I. N., Jones, K., and Dai, T. F., 1993, 3-D analytic signal in the interpretation of total magnetic field data at low magnetic latitudes. *Exploration Geophysics, 24*(4), 679-688.

Mapani, B. S. E., Rivers, T., Tembo, F., and Katongo, C., 2001, Terrane mapping in the eastern Irumide and Mozambique belts: Implications for the assembly and dispersal of Rodinia, in IGCP 418 4th Field Meeting, edited by S. McCourt, pp. 10 – 11, Univ. of Durban-Westville, Durban, South Africa.

Mapani, B., Rivers, T., Tembo, F., De Waele, B., and Katongo, C., 2004, Growth of the Irumide terranes and slices of Archaean age in eastern Zambia, paper presented at Geoscience Africa 2004, Geol. Soc. Of S. Afr., Johannesburg.

Mesko, G., Class, C., Maqway, M., Boniface, N., S. Manya, and S. Hemming (2014), The timing of early magmatism and extension in the southern East African Rift: Tracking geochemical source variability with 40Ar/39Ar geochronology at the Rungwe Volcanic Province, SW Tanzania, *In AGU Fall Meeting Abstracts.*

Michon, L., and Sokoutis, D., 2005, Interaction between structural inheritance and extension direction during graben and depocentre formation: An experimental approach, *Tectonophysics, 409*(1-4), 125-146.

Miller, H. G. and Singh, V, (1994), Potential field tilt – a new concept for the location of potential field sources, *Journal of Applied Geophysics, 32*.

Misra, A. A. and Mukherjee, S., 2015, Tectonic inheritance in continental rifts and passive margins. *Cham: Springer*.

Mondeguer, A., Ravenne, C., Masse, P., and Tiercelin, J., 1989, Sedimentary basins in an extension and strike-slip background; the" South Tanganyika troughs complex", East African Rift. *Bulletin de la Société géologique de France*, (3), 501-522.

Morley, C. K., 1989, Extension, detachments, and sedimentation in continental rifts (with particular reference to East Africa). *Tectonics, 8*(6), 1175-1192.

Morley, C. K., Cunningham, S. M., Harper, R. M., and Wescott, 1992, Geology and geophysics of the Rukwa rift, East Africa. *Tectonics, 11*(1), 69-81.

Morley, C. K., 1999, AAPG Studies in Geology #44, Chapter 1: Introduction to the East African Rift System, 1-18.

Mortimer, E., Paton, D. A., Scholz, C. A., Strecker, M. R., and Blisniuk, P., 2007, Orthogonal to oblique rifting: Effect of rift basin orientation in the evolution of the North basin, Malawi Rift, East Africa, *Basin Research, 19*, 393–407.

Mulibo, G. D., and Nyblade, A. A., (2016), The seismotectonics of Southeastern Tanzania: Implications for the propagation of the eastern branch of the East African Rift, *Tectonophysics, 674*, 20-30.

Njinju, E. A., 2016, Crustal and sub-continental lithospheric mantle decoupling beneath the Malawi Rift, Master of Science thesis, Oklahoma State University*, personal correspondence.*

Njinju, E.A., Atekwana, E.A., Stamps, D.S., Abdelsalam, M.G., Atekwana, E.A., Mickus, K.L., Fishwick, S., Kolawole, F., Rajaonarison, T.A. and Nyalugwe, V.N., 2019. Lithospheric structure of the Malawi Rift: Implications for magma-poor rifting processes. Tectonics, 38(11)

Nyalugwe, V.N., Abdelsalam, M.G., Atekwana, E.A., Katumwehe, A., Mickus, K.L., Salima, J., Njinju, E.A. and Emishaw, L., 2019. Lithospheric structure beneath the Cretaceous Chilwa Alkaline Province (CAP) in southern Malawi and northeastern Mozambique. Journal of Geophysical Research: Solid Earth, 124(11), pp.12224-12240.

Nyalugwe, V.N., Abdelsalam, M.G., Katumwehe, A., Mickus, K.L. and Atekwana, E.A., 2020. Structure and tectonic setting of the Chingale Igneous Ring Complex, Malawi from aeromagnetic and satellite gravity data: Implication for Precambrian terranes collision and Neogene-Quaternary rifting. Journal of African Earth Sciences, 163, p.103760.

Olsen, K.H. ed., 1995, Continental rifts: evolution, structure, tectonics. Elsevier.

Peace, A.L., Welford, J.K., Geng, M., Sandeman, H., Gaetz, B.D. and Ryan, S.S., 2018, Structural geology data and 3-D subsurface models of the Budgell Harbour Stock and associated dykes, Newfoundland, Canada. Data in brief, 21, pp.1690-1696.

Piper, D. P., 1989, Lineament analysis of the environs of the Malawi rift and the influence of pre-existing structures on rift morphology. *Journal of African Earth Sciences (and the Middle East), 9*(3-4), 579-587.

Ring, U., Betzler, C., and Delvaux, D., 1992, Normal vs. strike-slip faulting during rift development in East Africa: The Malawi rift, *Geology, 20*(11), 1015–1018.

Ring, U., 1994, The influence of preexisting structure on the evolution of the Cenozoic Malawi rift (East African rift system), *Tectonics, 13*, 303–326.

Ring, U., and Betzler, C., 1995, Geology of the Malawi Rift: Kinematic and tectonosedimentary background to the Chiwondo Beds, northern Malawi, *Journal of Human Evolution, 28*(1), 7-21.

Roberts, E.M., Stevens, N.J., O'Connor, P.M., Dirks, P.H.G.M., Gottfried, M.D., Clyde, W.C., Armstrong, R.A., Kemp, A.I.S. and Hemming, S., 2012, Initiation of the western branch of the East African Rift coeval with the eastern branch. *Nature Geoscience*, *5*(4), pp.289-294.

Samsu, A., Cruden, A.R., Micklethwaite, S., Grose, L. and Vollgger, S.A., 2020, Scale matters: The influence of structural inheritance on fracture patterns. Journal of Structural Geology, 130, p.103896.

Sander, S. and Rosendahl, B. R., 1989, The geometry of rifting in Lake Tanganyika, east Africa. *Journal of African Earth Sciences (and the Middle East), 8*(2-4), 323-354.

Sarafian, E., Evans, R.L., Abdelsalam, M.G., Atekwana, E., Elsenbeck, J., Jones, A.G. and Chikambwe, E., 2018, Imaging Precambrian lithospheric structure in Zambia using electromagnetic methods. Gondwana Research, 54, pp.38-49.

Saria, E., Calais, E., Stamps, D.S., Delvaux, D., and Hartnady, C.J.H., 2014, Present-day kinematics of the East African Rift. Journal of Geophysical Research: Solid Earth, 119(4), pp.3584-3600.Scholz, C.H., 2007. The scaling of geological faults. Earthquakes and Acoustic Emission

Schmeling, H., 2010, Crustal accretion at high temperature spreading centres: Rheological control of crustal thickness. Physics of the Earth and Planetary Interiors, 183(3-4), pp.447-455.

Scholz, C.A., Cohen, A.S., Johnson, T.C., King, J., Talbot, M.R. and Brown, E.T., 2011. Scientific drilling in the Great Rift Valley: the 2005 Lake Malawi Scientific Drilling Project—an overview of the past 145,000 years of climate variability in Southern Hemisphere East Africa. Palaeogeography, Palaeoclimatology, Palaeoecology, 303(1-4), pp.3-19.Specht, T. D., and B. R. Rosendahl (1989), Architecture of the Lake Malawi rift, east Africa, *Journal of African Earth Sciences*, *8*(2), 355–382.

Stamps, D.S., Calais, E., Saria, E., Hartnady, C., Nocquet, J.M., Ebinger, C.J. and Fernandes, R.M., 2008, A kinematic model for the East African Rift. Geophysical Research Letters, 35(5), Thybo, H. and Nielsen, C.A., 2009. Magma-compensated crustal thinning in continental rift zones. Nature, 457(7231), pp.873-876.

Tommasi, A. and Vauchez, A., 2001, Continental rifting parallel to ancient collisional belts: an effect of the mechanical anisotropy of the lithospheric mantle. Earth and Planetary Science Letters, 185(1-2), pp.199-210.Tommasi, A. and A. Vauchez (2015), Heterogeneity and anisotropy in the lithospheric mantle, *Tectonophysics, 661*, 11-37.

Toth, C. K., Koppanyi, D. A. Grejner-Brzezinska, and G. Jóźków, 2014, Spatial Spectrum Analysis of Various Digital Elevation Models, in *ASPRS Annual Conference, Louisville, KY.*

Van Wijk, J.W., 2005, Role of weak zone orientation in continental lithosphere extension, *Geophysical Research Letters, 32*(2).

Vauchez, A., Tommasi, A. and Barruol, G., 1998. Rheological heterogeneity, mechanical anisotropy and deformation of the continental lithosphere. Tectonophysics, 296(1-2), pp.61-86.

Versfelt, J., and Rosendahl, B**,** 1989, Relationships between pre-rift structure and rift architecture in Lakes Tanganyika and Malawi, East Africa, *Nature, 337*, 354–357.

Wedmore, L.N., Williams, J.N., Biggs, J., Fagereng, Å., Mphepo, F., Dulanya, Z., Willoughby, J., Mdala, H. and Adams, B., 2020, Structural inheritance and border fault reactivation during active early-stage rifting along the Thyolo fault, Malawi. Journal of Structural Geology, p.104097.

Wilson, R.W., 2006, Digital fault mapping and spatial attribute analysis of basement-influenced oblique extension in passive margin settings (Doctoral dissertation, Durham University).

Woolley, A. R., 1991, The Chilwa alkaline igneous province of Malawi: a review, in *Magmatism in Extensional Structural Settings,* 377-409. Springer, Berlin, Heidelberg.

Woolley, A. R., 2001, Alkaline rocks and carbonatites of the world, Part 3: Africa, *Geological Society of London, Natural History Museu* 372.

VITA

Kathleen E. Robertson

Candidate for the Degree of

Master of Science

Thesis: RIFT BRITTLE STRUCTURE, PRECAMBRIAN DUCTILE STRUCTURE, AND CRUSTAL THICKNESS VARIATION WITHIN AND AROUND THE CENOZOIC MALAWI RIFT

Major Field: Geology

Biographical:

Education:

Completed the requirements for the Master of Science in geology at Oklahoma State University, Stillwater, Oklahoma in December, 2020.

Completed the requirements for the Bachelor of Science in geology at Brigham Young University, Provo, Utah in 2013.

Experience:

Staff Geologist, Freestone Environmental Services, Inc., 2016-2018.

Geophysics Intern, ConocoPhillips, Summer, 2014.

Teaching Assistant: Physical Geology, Geomorphology, and Mineralogy, Oklahoma State University 2013-2014.

Teaching Assistant: Historical Geology, Geology for Engineers, Dinosaurs, Structural Geology and Field Mapping during Summer Field Camp, Brigham Young University 2010-2013.

Professional Memberships:

American Association of Petroleum Geologists, Association for Women Geoscientists, Geological Society of America, American Geophysical Union